4. General Discussion

4.1 Performance of the eddy correlation measurement system

Micrometeorological techniques provide a direct way to estimate of the heat, water and CO_2 exchanges between ecosystems and the atmosphere. They are in situ, have relatively large sampling area compared to the enclosures, and have little modification to the measured surfaces (Baldocchi, 1994a, b, 1997; Baldocchi and Meyer, 1988a, b; 1998). Of the micrometeorological techniques, the EC technique is most attractive since it does not strictly rely on the assumption, e.g. energy balance, similarity, and atmospheric stability functions although it requires an open, uniform and level surface, i.e. sufficient fetch as other micrometeorological techniques such as the profile method (Baldocchi et al., 1988, 1996, 2000; Dabberdt et al., 1993). When used to measure the fluxes of mass and energy over a canopy, the EC technique, like other micrometeorological techniques, requires that the canopy surface should be horizontally flat, homogeneous and extensive (i.e. sufficient scalar-sampling fetch) without obvious existence of advection for the scalars under investigation (e.g. Baldocchi et al., 1988; Lafleur et al., 1997; Schotanus et al., 1983; Schuepp et al., 1990). The instruments should be able to simultaneously capture the rapid fluctuations of vertical wind velocity, CO_2 and H_2O densities near the canopy surface at an adequate frequency (e.g., Dabberdt et al., 1993; Jarvis, 1995a; Leuning and King, 1992), and be adequately arranged in the field (e.g. Dabberdt et al., 1993; Lee et al., 1994; Lee and Black, 1994; Moore, 1986; Suyker and Verma, 1993). Therefore, it is necessary to evaluate the reliability of the EC measurement system. One method is to check the closure of the surface energy budget components, i.e. examine whether or not the sum of the latent heat and sensible heat fluxes equals the available energy (Baldocchi and Harley. 1995).

In the present study, we use the energy balance closure check to assess the performance of our EC measurement system; we also make the comparison between the EC-measured *LE* and the lysimeter-measured *LE*. Ideally, Q_n should be balance by the sum of the eddy fluxes of *H* and *LE*. Examination of the closure of the surface energy budget components indicates that the sum of sensible heat and latent heat flux densities measured with the EC technique matched the available energy flux density satisfactorily over most of the measurement period (Fig. 13). The slope of the relationship between Q_n and its partitioned components ($H + LE$) was 1.01 on the hourly averaged basis and 1.04 on the daily averaged basis. This favorable closure of the canopy surface energy budget demonstrates that measurement accuracies associated with our EC measurement system were quite satisfactory and this system was reliable in estimating eddy fluxes. A comparison between the hourly averaged latent heat flux density estimated by the EC technique and those measured directly by the lysimeter indicates they were fairly consistent (Figs. 15 to 16).

However, imbalance of the energy budget was found during the senescence period of grasses. Hourly energy budget closure was only about 0.42 for this period. This point is also indicated in the daily energy budget closure check (Fig. 14). At least part of this energy imbalance may be attributable to differences in sampling areas for the eddy flux and available energy measurements (Hollinger et al., 1994; Kelliher et al., 1997; Valentini et al., 1995). Lack of closure may also arise from other factors, for example, inaccuracy and poor array of instruments (Lee and Black, 1994), and atmospheric stability (Blanken et al., 1997). Partly cloudy conditions resulted in 15% underestimation in $H + LE$ for 5 consecutive days during the closed canopy period and 27% overestimation of $H + LE$ for 8 intermittent days during the flowering period.

Theoretically, an adequate fetch should be guaranteed in use of the EC technique (Horst, 1999; Laubach et al., 1994; Stannards, 1997). McMillen (1988) argues that larger uniform fetches appear to be necessary over smooth surfaces and/or in stable conditions than over rough surfaces (e.g. forests) and/or under unstable conditions. However,

Savage et al. (1996) drew a contrary conclusion that the fetch requirement for micrometeorological measurements above a forest canopy is more stringent than that for a grassland canopy. Heilman et al. (1989) even suggested that the Bowen ratio method can be used successfully even at fetch-to-height ratios as low as 20:1. Does fetch affect the closure of the energy balance in the present study? How far is far enough for a fetch in the present study? To answer those questions, we plotted the ratio of $(H + LE)/(R_n - G)$ against the fetch-to-height ratio (Fig. 28a). Most points during the measurement period except for the senescent period were concentrated within 20% of unity (acceptable closure). Closure increased with increase of the fetch-to-height ratio. Most scatter in Fig. 28a was from the measurements during the senescent period. Phenological heterogeneity in this period, which could be caused by both the patch-like aging of C3/C4 grasses and the abrupt change in height of individual species due to flowering growth of *Solidago altissima* (C3) and *Miscanthus sinensis* (C4), made EC sensors sample different sources from those sampled by radiation sensors. This heterogeneity may also give rise to changes in canopy surface albedo (Fig. 6b). Since DOY 291, air temperatures were often less than the biotic frost temperature (<5 °C), which further enhanced the heterogeneity. In other words, the canopy surface became much rougher both in phenology and in physiognomy during the senescent period. Furthermore, northeast wind direction dominated the later part of the senescent period, which may also contribute to an incomplete closure of the energy balance (Fig. 28b). Thus, poor fetch may affect markedly the closure of energy balance. We strongly recommend a fetch-to-height ratio exceeding at least 50:1 for the present study of grassland eddy fluxes.

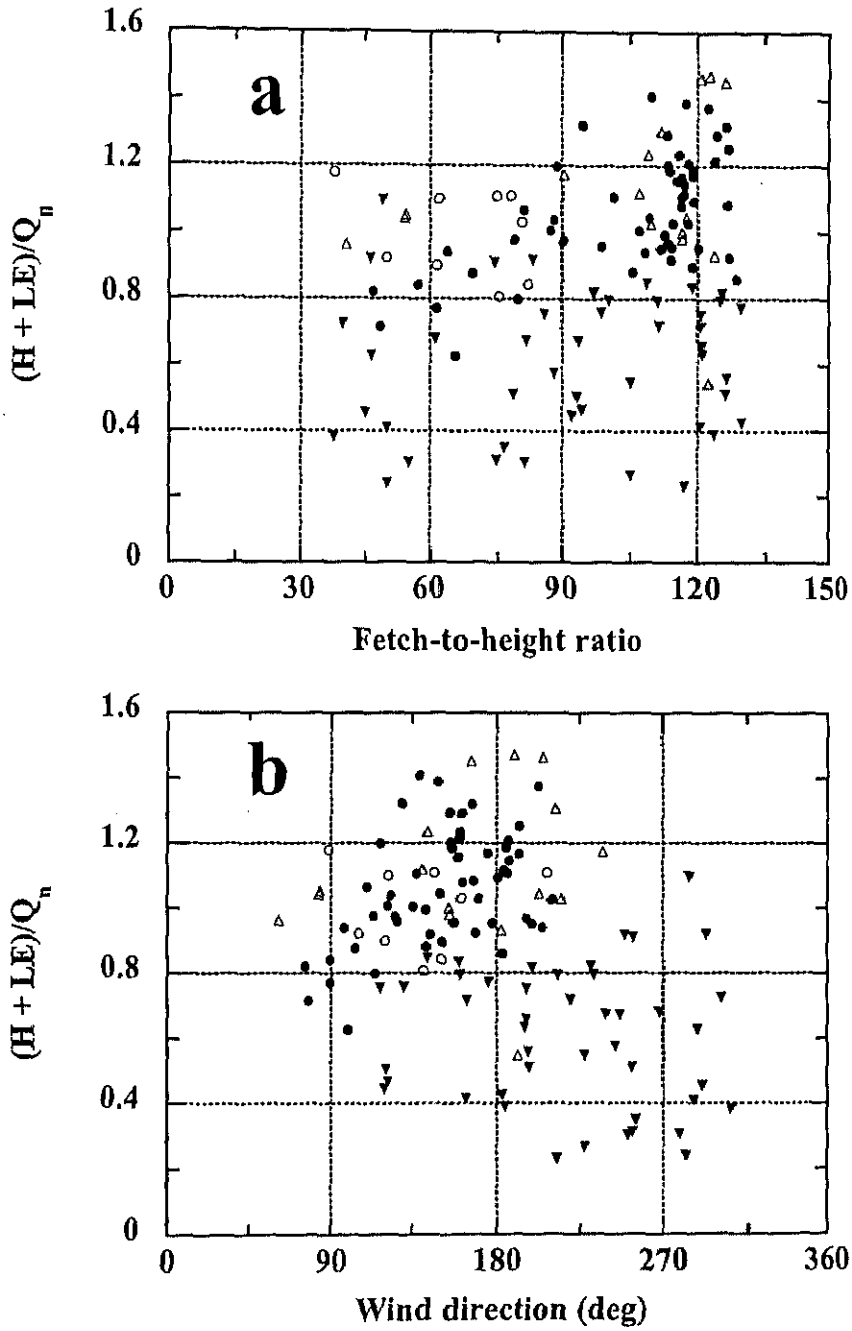

Figure 28. a: Relationship between energy balance closure and fetch-to-height ratio. b: Relationship between energy balance closure and wind direction. The data were grouped according to the growth stages of grasses: the period prior to closed canopy (○), the closed canopy period after the *Baiu* rainy season and before flowering (●), the flowering period (△), and the senescence period (▼).

4.2. Determinants for the available energy-partitioning pattern

It is commonly thought that the partitioning pattern of the available energy is principally governed by such environmental factors as solar radiation, soil and air temperatures, wind regime, soil water availability, ecophysiological features of plants, and canopy architecture (LAI, species composition, phenology, etc.) (e.g. Baldocchi, 1994a, Baldocchi et al., 1997a, Kelliher et al., 1993). During the measurement period, volumetric soil water content was generally larger than 0.35, indicating that the ERC grassland was not water restricted and that soil moisture was a main determinant but not a limiting factor for the partitioning of the available energy. Diurnal and seasonal variations in LE were strongly coupled with diurnal and seasonal variations in Q_n, suggesting that Q_n is one major determinant for dynamics of LE (Figs. 17 to 21 and Table 2). For most of the measurement period, more than 70% of LE can be explained by variations in Q_n (linear regression: $LE = 0.60Q_n + 20.27$, $n = 2418$ h, $r^2 = 0.79$). A linear relationship was also established between LE and VPD ($LE = 134.8$VPD, $n = 2418$ h, $r^2 = 0.66$), which could be explained by the fact that LE and VPD behaved in a parallel fashion in daily variations. Linear relationships between LE and wind speed, u and air temperature, T_a at a height of 1.6 m were not clear in the present study ($r^2 = 0.30$ for u and $r^2 = 0.20$ for T_a) for the same period. The influence of air temperature on the partitioning of the available energy was generally reflected in variations in VPD. Generally, LE increases with increasing VPD and T_a when soil moisture is nonlimiting (Jarvis and McNaughton, 1986). This pattern is modulated by conductances (Jarvis and McNaughton, 1986).

McNaughton and Jarvis (1983) and Jarvis and McNaughton (1986) introduce the so-called omega factor (Ω) to evaluate coupling of the canopy surface to outer environmental conditions, or the capacity of a canopy to exchange heat and mass with

the air including pattern of partitioning of the available energy. A value of Ω close to 1 implies that the canopy decouples from the atmosphere and LE is controlled by Q_n while a value of Ω close to 0 indicates that the degree of coupling between the canopy and the atmosphere is fairly strong and LE is regulated by the stomata (McNaughton and Jarvis, 1983; Jarvis and McNaughton, 1986). Figs. 29 and 30 presents daily courses of Ω, Bowen ratio (β), dryness index (DI), and Priestley-Taylor coefficient (α, P-T parameter) and several meteorological variables for the selected days from DOY 151 to 159 during the rapid growth period and for the selected clear days from DOY 204 to 216 during the closed canopy period. Similar data are available for the other growing periods but are not presented here graphically.

Values of Ω peaked (0.95) in the mid-morning hours, decreased from morning through afternoon, and reached the daytime minimal value of about 0.10 in late afternoon. This is associated with the daytime trends in g_a and g_c (Fig. 32). Midday (09:00 to 14:00 JST) mean values of Ω were *ca.* 0.77 ($\pm$ 0.09 SD). According to McNaughton and Jarvis (1983) and Jarvis and McNaughton (1986), higher values of Ω in the morning imply that the canopy was decoupled from the atmosphere, and that latent heat flux (evapotranspiration) was controlled by the available energy. Lower values of Ω in the afternoon demonstrate that the canopy was coupled to the atmosphere and that evapotranspiration from the canopy surface is regulated primarily by VPD and canopy surface conductance except for the available energy. In other words, the "imposed" evapotranspiration contributed relatively more to water loss from the canopy surface than the equilibrium evapotranspiration in the afternoon as compared to the morning. Similar patterns of Ω factor are reported in Steduto and Hsiao (1998a) for maize, and in Köstner et al. (1992) for a red beach forest.

Transition from decoupling in the morning hours to coupling in the afternoon hours is explainable by both the relative increase in the atmospheric evaporative demand (VPD) and the sensible heat advection in the afternoon. As we stated before, soil moisture is ample for the ERC grassland during the measurement period. As a result of

full absorption of water from the soil the previous night, water in grasses was sufficiently plentiful in the morning to meet the atmospheric evaporative demand. Omega factor analysis, however, indicates there was actually a slight water stress in the afternoon. Therefore, we could reasonably suspect that amount of water abstracted from the soil by roots of grasses and/or hysteresis in water take-up in the afternoon were responsible for the deepening of apparent water stress due to much consumption of water by grasses. This pattern is modulated by variations in the canopy surface conductance because higher Ω values were generally linked with higher canopy surface conductance values (data not presented here), i.e. higher canopy surface conductance in the morning was favorable to decoupling. Obviously, the sensible heat advection (SHA) intensified (Figs. 29a and 30a) this water restriction scenario by adding energy to evaporating water, because SHA was commonly associated with both comparatively higher temperatures (or VPD) and stronger winds (Figs. 29b and 30b) (Rosenberg et al., 1983). SHA may be one of the major determinants for decrease of Ω in the late afternoon. As argued in Steduto and Hsiao (1998a) and Kelliher et al. (1993), higher winds (stronger turbulent mixing) and corresponding larger aerodynamic conductance, and relatively lower canopy surface conductance in the afternoon enhance coupling. Higher aerodynamic conductance may lead to a higher Ω value (Verma et al., 1986).

Midday (09:00 to 14:00 JST) mean Ω values were generally larger than 0.6 throughout the growing season (Table 5), implying that the ERC grassland was decoupled from the atmosphere and the canopy-atmosphere water exchange was mainly dependent on the available energy in the growing season. This result is comparable to the values (about 0.7 to 0.8) reported by McNaughton and Jarvis (1983) and Jarvis and McNaughton (1986) for grasslands and crops. With progression of the growing season, Ω tended to decrease, indicating the grassland canopy tended to couple with the atmosphere and *ET* was much more regulated by the canopy surface conductance. Midday mean Ω values diminished to about 0.7 during the flowering period and the

senescent period. This may be very possibly due to patch-like heterogeneity caused by abrupt growth for flowering of several species that made the canopy surface aerodynamically rougher. This point could also be explained in terms of the drop of canopy surface conductance in the later growing seasons as suggested by Steduto and Hsiao (1998a). Valentini et al. (1995) reported a similar seasonal pattern of Ω factor for a serpentine grassland in which vales of Ω vary from 0.8 (poor couple) at an early growth stage to 0.1 (perfect couple) at a later growth stage.

The Priestley-Taylor coefficient (α) was calculated as the ratio of the residual of energy balance ($LE = R_n - G - H$) to the equilibrium evapotranspiration. As shown in Figs. 29a and 30a, values of α were constant in daytime except for mid-morning and late afternoon hours. Higher values of α in the mid-morning may be due to evaporation of dew while those in the late afternoon may be caused by the sensible heat advection that increased evapotranspiration from the canopy surface (Monteith, 1995). Mean α values were larger than unity throughout daytime, indicating that the ERC grassland was not water limited and the canopy-atmosphere water exchange was controlled by environmental factors other than soil moisture. Midday α values at different growing periods are presented in Table 5.

As illustrated in Figs. 29a and 30a, dryness index (DI, expressed as LE/R_n, Smith et al., 1992) was lower in the morning and increased in the afternoon. The reverse pattern was observed for the Bowen ratio (β). β approached peak values in the mid-morning, decreased first slowly, and then precipitously at around 16:00 JST. Daily values of DI generally ranged between 0.5 and 1.0; increase in DI in the afternoon hours means the deepening of water stress or a steeper VPD between the canopy surface and the air. The mid-morning higher values of β are consistent both with lower H due to low winds and with larger ET as a result of evaporation of dew. Lower values of VPD in the morning hours may also contribute to this pattern (Jarvis et al., 1997). The decline in β throughout the afternoon hours is reasonably attributable to asymmetrical or asynchronous decrease of H and LE caused, evidently, by the sensible heat advection

(Figs. 29a and 30a) (Kim and Verma, 1990a). The seasonal pattern of β presented in Table 2 indicates that β was lower after the canopy closed and increased with decrease of evaporative ability of grasses due to senescence. When the canopy entered the senescent period, β was generally greater than unity because a larger part of Q_n was partitioned into H.

Cloudiness could modulate the daily course of the available energy-partitioning pattern. The sensible heat advection was not clear on very cloudy days largely because of the lack of apparent water stress on those whole days due to diminishment of evapotranspiration (smaller solar energy gain).

Additionally, canopy architecture, which is indicated by LAI, affects evapotranspiration substantially. Evapotranspiration (ET) generally increases with LAI up to a value of *ca.* 3 when soil moisture is not limited (Rosenberg et al., 1983). For the present study, ET could increase with LAI before the canopy closed. Unfortunately, we could not test this prediction because of instrument malfunction. Since the canopy remained closed until the senescent period, it seemed that ET was not closely coupled to LAI, as shown in Table 1. The reason might be that ET was restricted not by soil moisture but by energy gain, as suggested by Stewart and Verma (1992). It may be also true that ET was controlled by effective LAI (or evaporative ability of grasses) rather than the apparent LAI estimated by the canopy analyzer for the period from the closed canopy through the senescence.

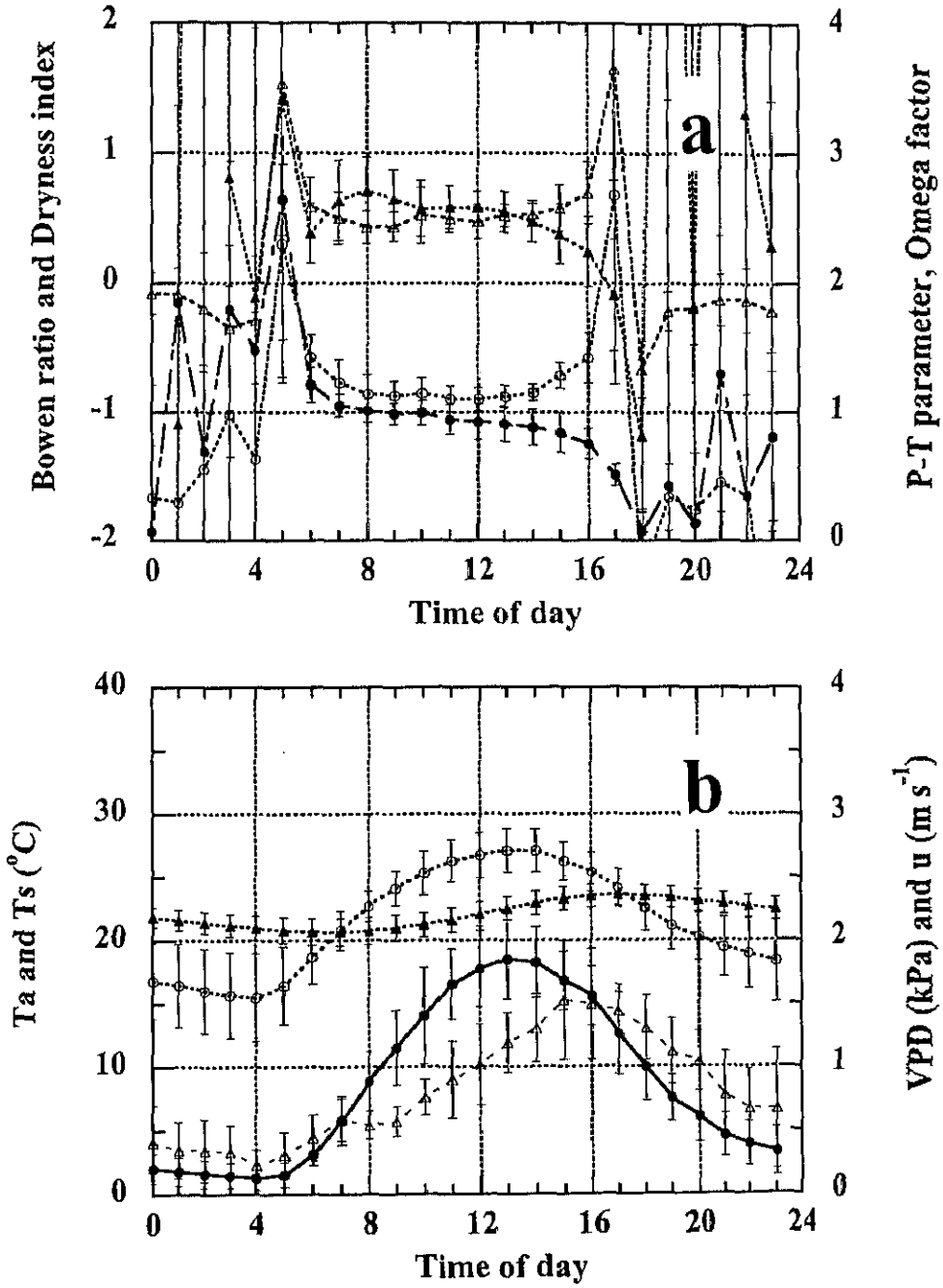

Figure 29. a: Daily variations in omega factor (Ω, ●), the Priestley-Taylor coefficient (α, P-T parameter, ○), the Bowen ratio (β, ▲), and dryness index (DI, △). b: Daily variations in air temperature at 1.6 m (T_a, ○), soil temperature at depth of 2 cm (T_s, ▲), vapor pressure deficit (VPD, ●), and wind speed at 1.6 m (u, △). Data are hourly averages over the selected days from DOY 151 to 159 during the rapid growth period. Vertical bars in the figure indicate standard deviations. Note that Ω and α were computed from the routine meteorological observations at the MOT.

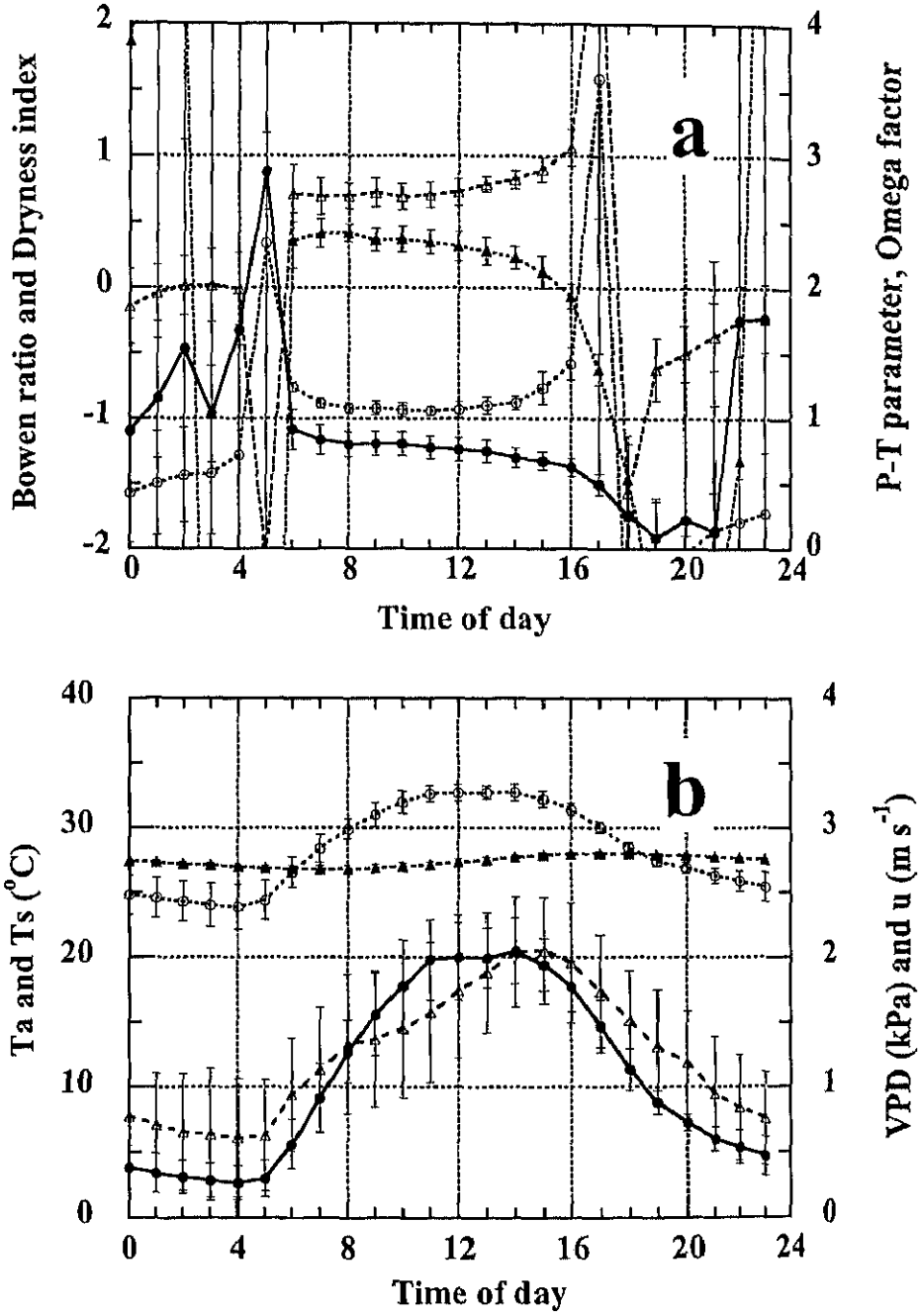

Figure 30. Same as Fig. 29 but for the selected days from DOY 204 to 216 during the closed canopy period.

Table 5 Mean values of leaf area index (LAI), the Bowen ratios (β), midday (09:00-14:00 JST) mean values of omega factor (Ω) and Priestley-Taylor coefficient (α), and midday mean aerodynamic conductances (g_a), midday mean canopy surface conductances (g_c) in various growth periods of the ERC grassland in 1999. Values in parentheses are standard deviations.

Period	DOY	LAI	β	Ω	α	g_a	g_c	g_s
							mm s^{-1}	
Prior to canopy closure	151–159 (8d)	2.13	0.60	0.91 (±0.07)	1.10 (±0.07)	10.5 (±2.4)	18.8 (±9.5)	11.2 (±5.4)
Closed canopy	204–216 (13d)	5.25	0.32	0.77 (±0.09)	1.08 (±0.05)	31.9 (±9.8)	21.9 (±8.1)	5.3 (±2.0)
Closed canopy	227–235 (9d)	5.50	0.38	0.84 (±0.05)	1.13 (±0.14)	22.5 (±7.2)	23.3 (±6.0)	5.3 (±1.4)
Closed canopy (Cloudy days)	236–240 (5d)	5.50	0.46	0.87 (±0.06)	1.17 (±0.08)	18.7 (±3.9)	30.2 (±12.6)	6.8 (±2.8)
Closed canopy	241–255 (15d)	5.50	0.59	0.80 (±0.07)	1.10 (±0.15)	21.4 (±7.1)	19.9 (±6.8)	4.5 (±1.5)
Flowering	271–290 (11d)	5.37	1.17	0.70 (±0.10)	0.97 (±0.10)	18.8 (±7.7)	11.9 (±3.8)	2.7 (±0.9)
Flowering (Cloudy days)	271–290 (8d)	5.37	0.80	0.88 (±0.14)	1.35 (±0.31)	12.8 (±6.2)	28.9 (±25.2)	6.7 (±5.9)
Senescence	291–304 (8d)		1.20	0.68 (±0.14)	1.03 (±0.06)	20.1 (±15.5)	9.6 (±2.3)	2.4 (±0.6)
Senescence	310-318 (8d)		1.76	0.67 (±0.19)	1.01 (±0.25)	15.3 (±5.0)		

4.3 Determinants for the net canopy CO_2 flux density

4.3.1 F_c in relation to ET

Because of their common dependence on incident energy (PPFD or Q_n) and their same mechanisms to communicate with the air via stomata, we expected that F_c and ET be linearly related with a high coefficient of determination (Fig. 31). Diurnal trends in F_c and ET usually paralleled each other at the ERC grassland. Therefore, the factors determining ET regime would affect F_c at the same time. Omega factor (Ω) analysis for ET stated above might be extended to the case for F_c. Like ET, F_c was determined primarily by the Q_n throughout the growing season at the ERC grassland because midday Ω values were generally greater than 0.7. On a daily basis, since midday Ω values were higher than 0.5 in the morning and declined in the afternoon, F_c was mainly controlled by Q_n in the morning and was affected by other factors such as VPD and SHA other than Q_n in the afternoon.

The slope (3.46 mg CO_2 g-1 H_2O) of the linear relationship of F_c and ET can be considered to be a surrogate for the average WUE of the canopy for the entire measurement period. This value is fairly smaller than the midday mean value of WUE at different growth stages, which varied between 12 and 19 mg CO_2 g-1 H_2O (Table 4). This can be explained by the fact that WUE was rather small during the afternoon hours due to the combined effect of high VPD and SHA (Fig. 27), which resulted in more water consumption relative to the morning. The linear relationship between F_c and ET varies dependent on the growth stage. The slope was 4.45 (r^2 = 0.83) for the rapid growth period, 3.62 (r^2 = 0.73) for the early part of the closed canopy period, 4.40 (r^2 = 0.59) for the later part of the closed canopy period, 3.92 (r^2 = 0.28) for the flowering period, and 2.61 (r^2 = 0.46) for the senescent period, respectively.

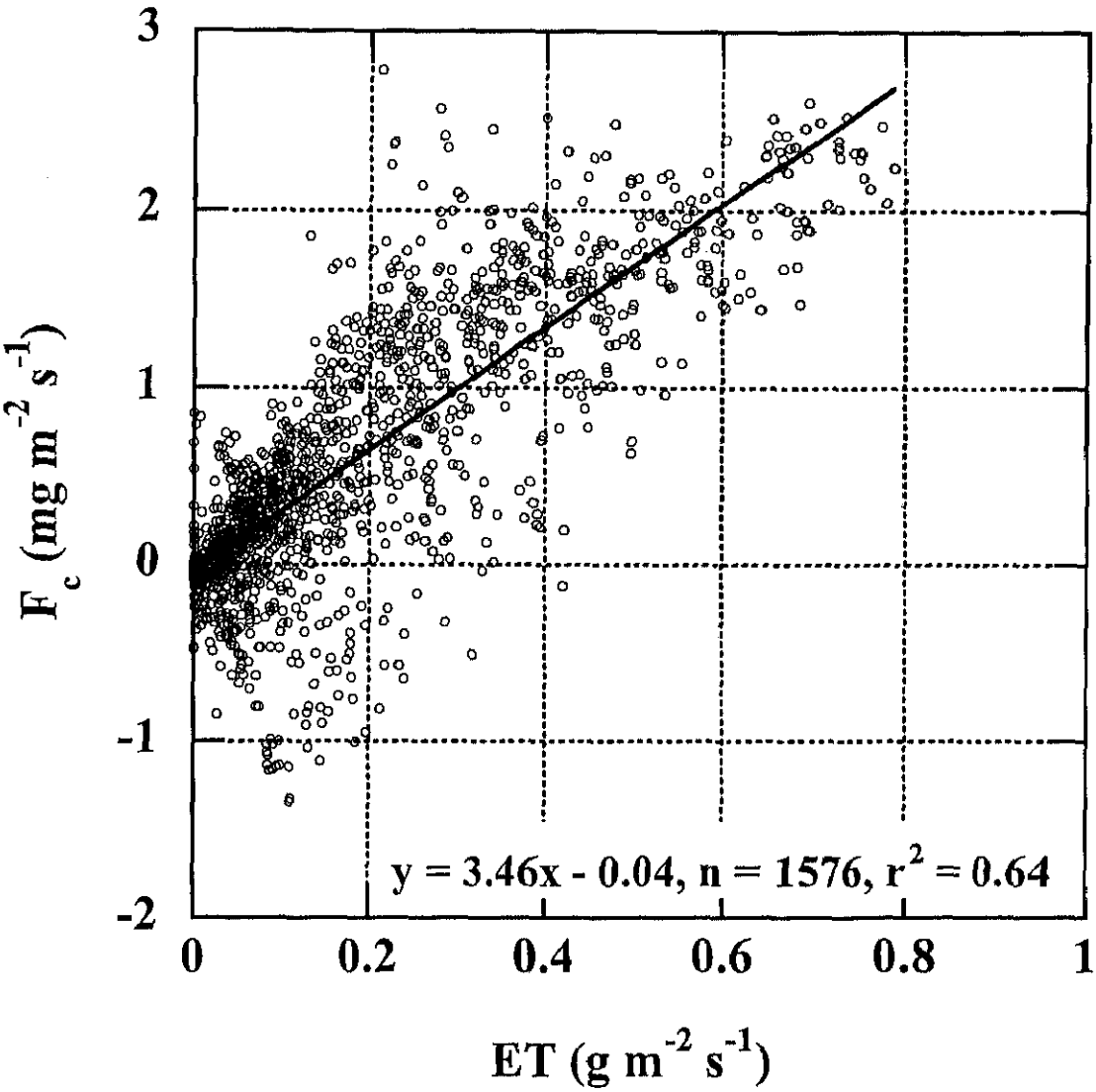

Figure 31. The relationship between net canopy CO_2 flux (F_c) and canopy evapotranspiration (ET) in daytime. F_c and ET were measured by the EC technique. The regression line is: F_c (mg m^{-2} s^{-1}) = 3.46 ET (g m^{-2} s^{-1}) – 0.04, n = 1576, r^2 = 0.64.

4.3.2 Dependence of F_c on canopy surface conductance

Canopy surface conductance (g_c) is one of the major factors determining the partitioning of available energy over the canopy as well as the net canopy CO_2 flux density, F_c (Jarvis and McNaughton, 1986; Monteith, 1995). Roles played by g_c in the partitioning of available energy were discussed through its coupling with omega factor (a higher value of omega factor is often associated with a higher conductance) in section 4.2. Here we present its effect on F_c.

Clear diurnal trends in canopy surface conductance, g_c and stomatal conductance, g_s (when $Q_n > 0$, the same hereafter) were observed (Fig. 32). The g_c and g_s generally approached their peak values in the mid-morning (07:00 to 10:00, JST) and declined with time throughout the remainder of the daytime. Higher values of g_c and g_s in the midmorning may be due to optimal water status within plant bodies as a result of sufficient absorption of water from the soil during the previous night. Lower values of g_c and g_s (partial stomatal closure) in the late afternoon may be attributable to higher atmospheric evaporative demand that exceeds water supply from the soil (occurrence of water stress) (McNaughton and Jarvis, 1983). Sensible heat advection (SHA) may stimulate stomatal closure (rapid decline in g_c and g_s) through exasperating water stress due to its enhancement of evapotranspiration. SHA may also be responsible for inability of g_c recovery in the late afternoon. In addition, lower canopy surface conductance may be also related to lower solar radiation in the late afternoon (Kim et al., 1989). The diurnal patterns of g_c and g_s reported here are consistent with the observations of Grace et al. (1995b) for an Amazonia tropical forest, Miranda et al. (1997) for a cerrado savanna, and Steduto and Hsiao (1998a) for two maize canopies.

Diurnal patterns of g_c and g_s were independent of that of aerodynamic conductance, g_a, suggesting that they were controlled by different mechanisms in that g_c and g_s were mainly controlled by VPD while g_a was closely coupled with wind and aerodynamic

roughness of the canopy. g_a ranged from 10 to 40 mm s^{-1} in daytime and generally peaked in the afternoon since both wind speed and VPD were higher then. g_a was generally lower (less than 10 mm s^{-1}) at night due to lower wind speeds and commonly stable conditions (Fig. 32). g_a was usually higher than g_c, especially in the afternoon (Fig. 32). Aerodynamic conductances for the ERC grassland were similar to those for agricultural crops and grasslands (20 to 50 mm s^{-1}) reported by Jarvis (1981).

The similar diurnal patterns for g_c, g_s and g_a maintained throughout the growing season. However, they were often disrupted by cloudiness. Canopy conductance was generally higher on cloudy days than on clear days (Table 5). This may be primarily in response to decreasing VPD on cloudy days. Midday means of g_c and g_s decreased as the growing season progressed (Table 5). Seasonally, g_c varied from 9.6 mm s^{-1} in the senescent period to 23.3 mm s^{-1} in the early closed canopy period on clear days while g_s varied from 2.4 mm s^{-1} in the senescent period to 11.2 mm s^{-1} in the rapid growing period. We expected g_c in the late growing season to be governed by the photosynthetic capacity. Our results for g_c and g_s are comparable to the maximal canopy surface conductance (17.0 ± 4.7 mm s^{-1}) and maximal stomatal conductance (8.0 ± 4.0 mm s^{-1}) for temperate grassland, but smaller than the maximal canopy surface conductance (32.5 ± 10.9 mm s^{-1}) and maximal stomatal conductance (11.0 mm s^{-1}) for crops (Kelliher et al., 1995). A range of 10 to 25 mm s^{-1} of g_c was reported for a tallgrass prairie (FIFE) with maximal LAI = 3.2 (Kim and Verma, 1990a; Stewart and Verma, 1992).

Canopy surface conductance is sensitive to incident photosynthetic photon flux density (PPFD) and vapor pressure deficit (VPD) (Jarvis and McNaughton, 1986; Jones, 1992). Irrespective of the growth stage of the canopy, the responses of g_c to PPFD at various VPDs seemed to be described by an exponential relationship (Fig. 33) because the ERC grassland was not water-stressed throughout the growth season. Magnitude of g_c increase with increasing PPFD was dependent on VPD. Under lower VPD, the magnitude was higher (Fig. 33). The scatter in g_c vs. PPFD data was significant under lower PPFD and VPD, which may be associated with in situ microenvironmental

conditions (e.g. growth status of the grasses and water stress).

As stated above, both Bowen ratio and omega factor values declined in the late afternoon, which was consistent with trends of g_c and g_s but inverse to those for g_a; therefore, eddy fluxes (latent heat and CO_2 flux densities) were very reasonably determined by g_c or g_s rather than g_a. F_c tended to increase with increase of g_c, but the magnitude of increase depended on air temperature regime (Fig. 34). As air temperature exceeded 30 °C, F_c was very sensitive to g_c. F_c increased as g_c increased to a critical value of *ca.* 25 mm s^{-1} and it decreased as g_c exceeded that value. Responses of F_c to g_c also depended on VPD regime (Fig. 35). Increasing VPD seemed to enhance F_c although g_c was somewhat reduced. Effect of partial stomatal closure on F_c only occurred at relatively higher VPD values ($\geq$ 2 kPa). The ERC grassland was dominated by C4 grasses and experienced no water stress, so that higher g_c accompanied by higher air temperature and corresponding higher VPD may enhance atmospheric CO_2 fixation by the canopy.

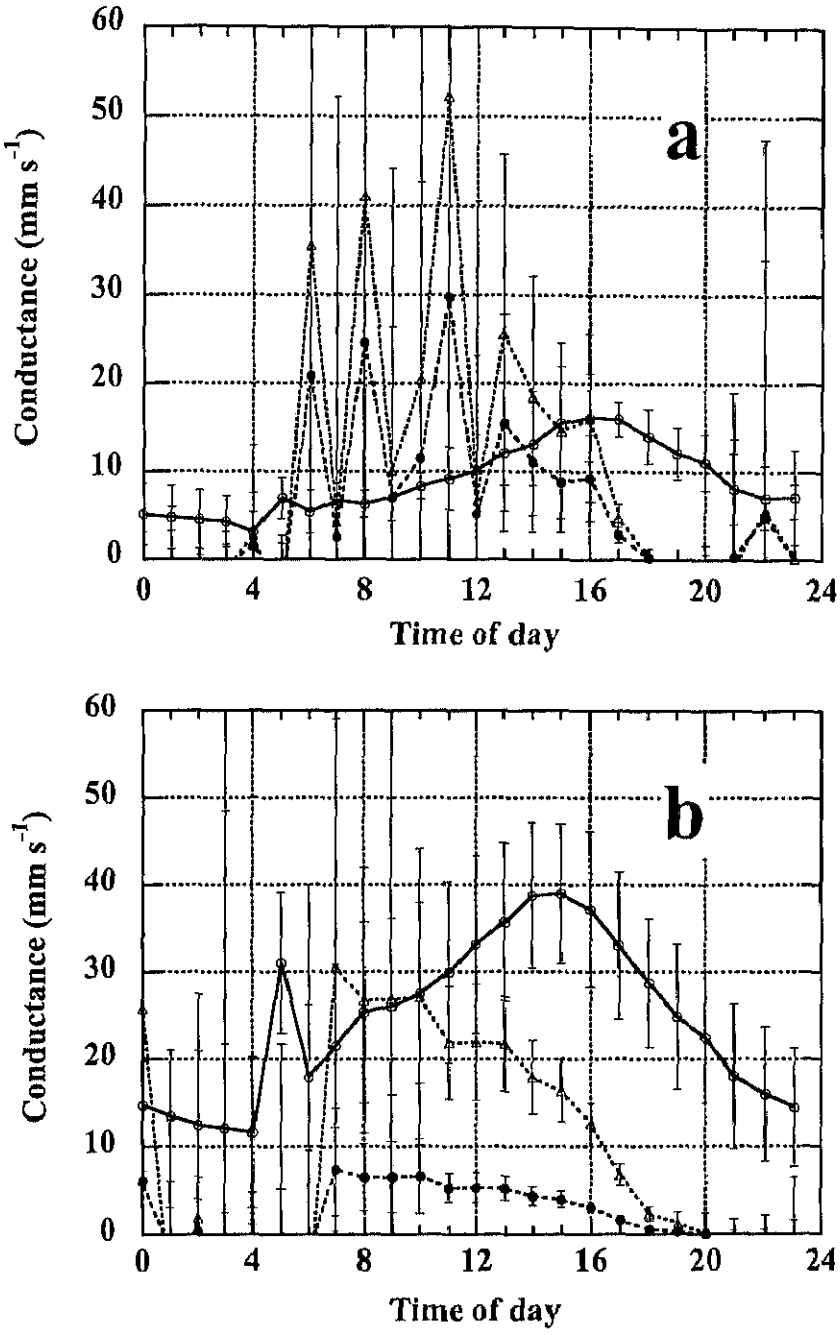

Figure 32. Diurnal trends in aerodynamic conductance (○), canopy surface conductance (△) and stomatal conductance (●) for selected clear days. a: the period prior to canopy closure (DOY 151 to 159, 9 days, LAI = 2.13). b: the closed canopy period (DOY 204 to 216, 13 days, LAI = 5.25).

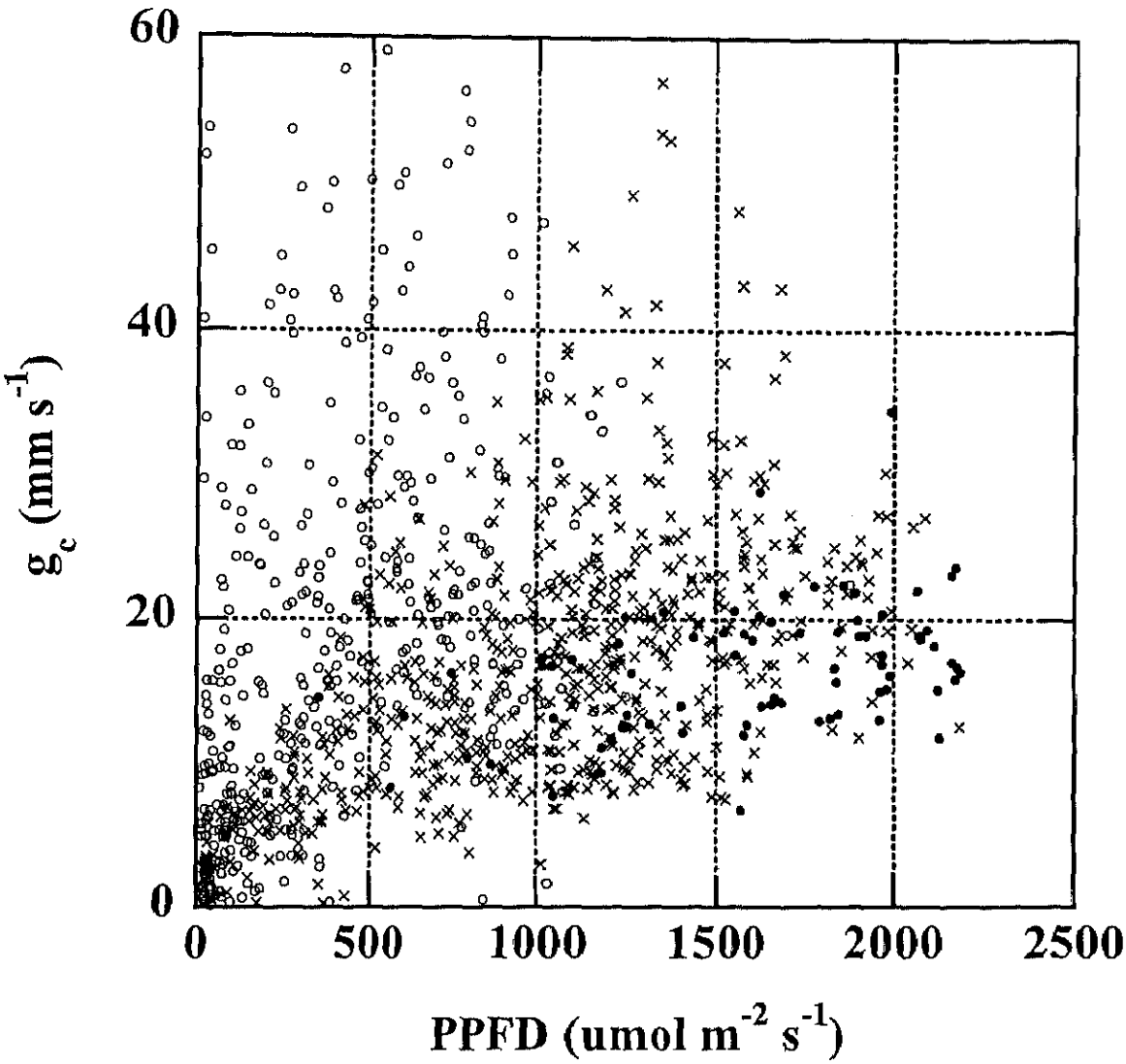

Figure 33. The relationship between canopy surface conductance (g_c) and photosynthetic photon flux density (PPFD) with respect to vapor pressure deficit (VPD). Lines of best fit are $g_c = 3.05\text{PPFD}^{0.31}$, $n = 844$, $r^2 = 0.19$ for VPD < 1 kPa (○), $g_c = 0.50\text{PPFD}^{0.51}$, $n = 648$, $r^2 = 0.32$ for $1 \leq \text{VPD} < 2$ kPa (×), and $g_c = 1.02\text{PPFD}^{0.38}$, $n = 84$, $r^2 = 0.18$ for VPD ≥ 2 kPa (●).

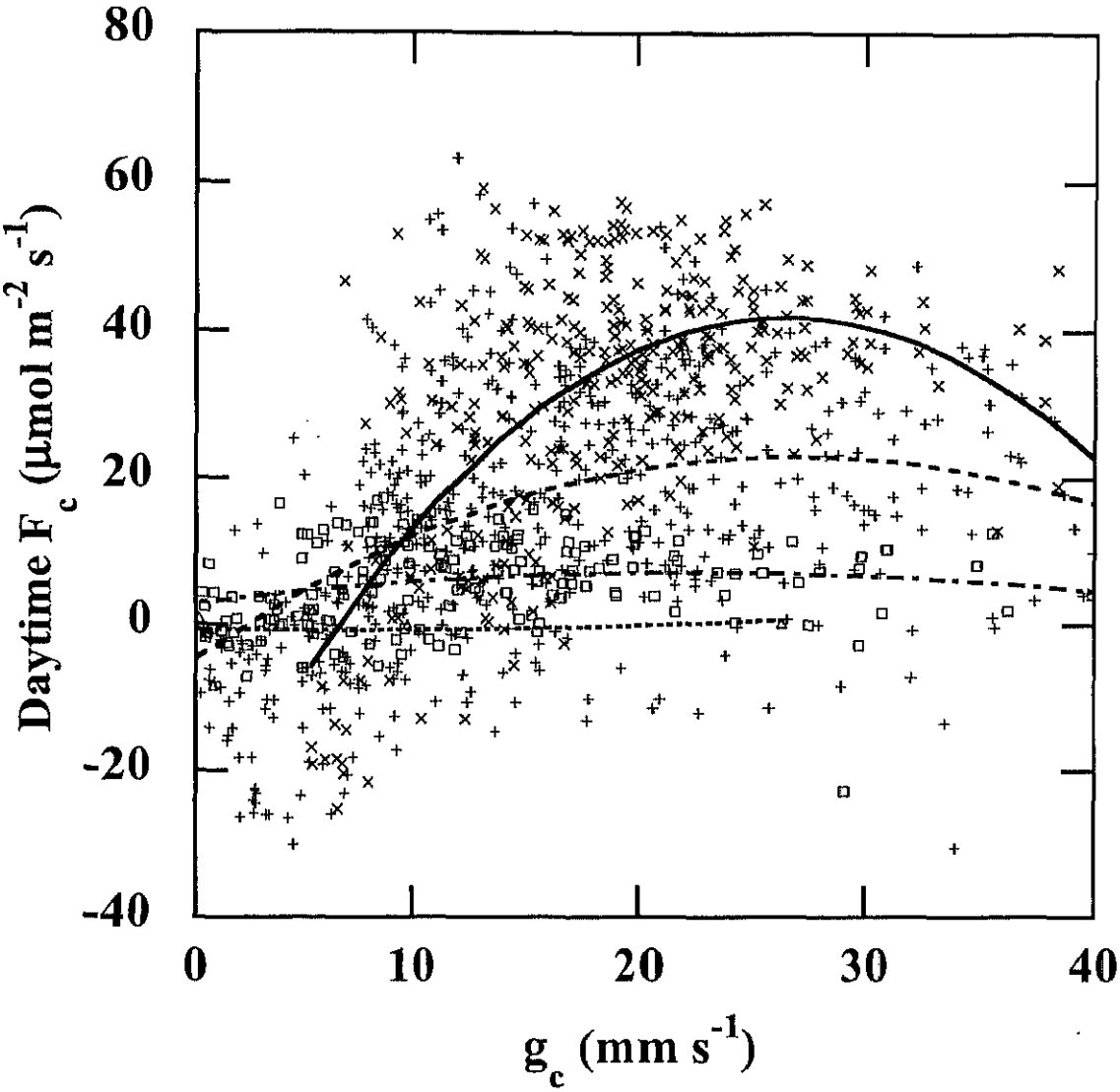

Figure 34. The relationship between the canopy CO_2 flux (F_c) and the canopy surface conductance (g_c) at various air temperature ranges (T_a) at 1.6 m. Lines of best fit are $F_c = -0.66 - 0.051\ g_c + 0.0039\ g_c^2$, $n = 44$, $r^2 = 0.01$ for $T_a < 10$ °C (△); $F_c = 2.85 + 0.377 g_c - 0.0083 g_c^2$, $n = 391$, $r^2 = 0.15$ for $10 \leq T_a < 20$ °C (□); $F_c = -4.68 + 2.049 g_c + 0.0379 g_c^2$, $n = 819$, $r^2 = 0.28$ for $20 \leq T_a < 30$ °C (+); and $F_c = -32.35 + 5.594 g_c - 0.1054 g_c^2$, $n = 322$, $r^2 = 0.40$ for $T_a \geq 30$ °C (×); respectively.

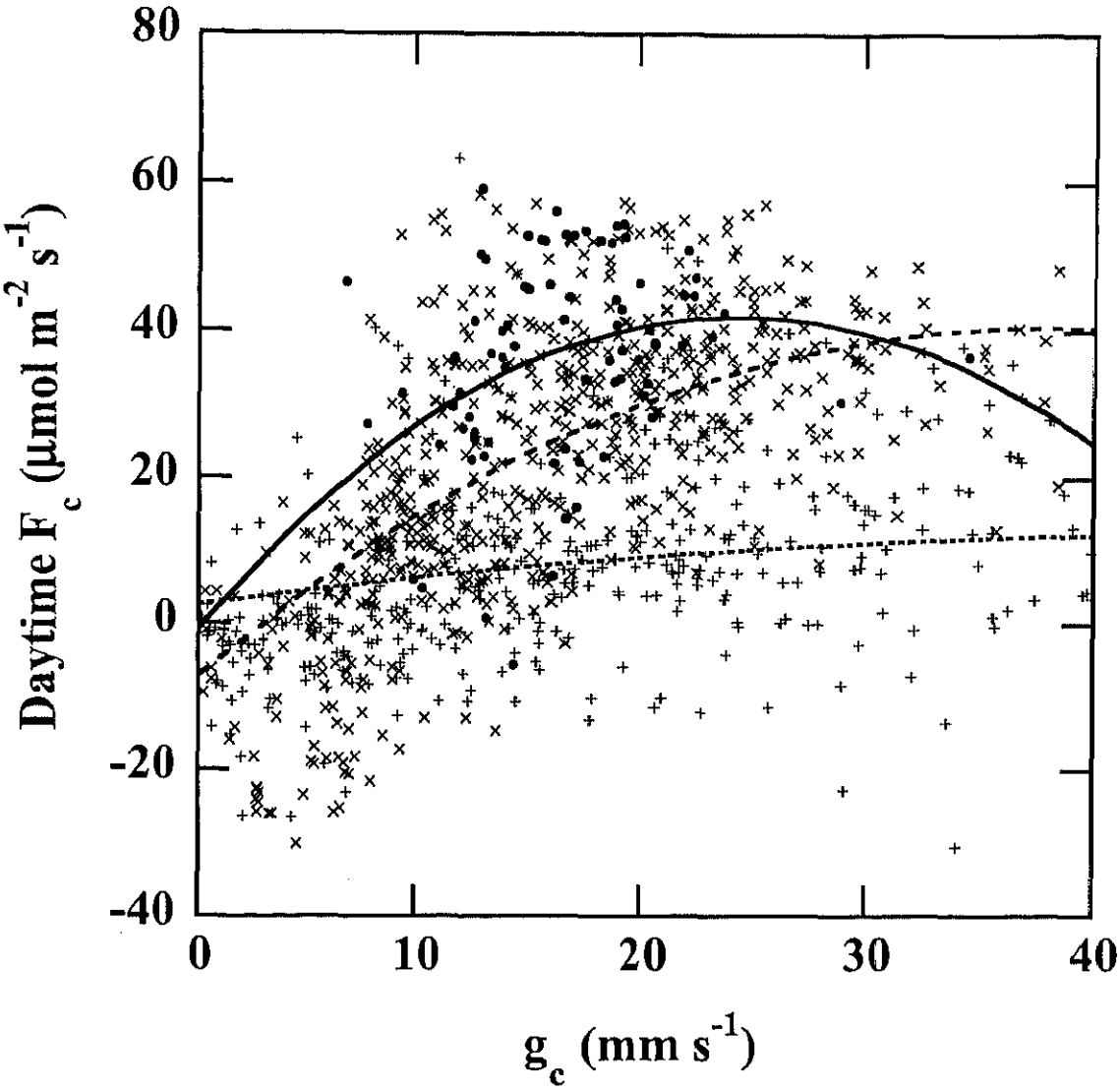

Figure 35. The relationship between the canopy CO_2 flux (F_c) and the canopy surface conductance (g_c) at various vapor pressure deficit ranges (VPD) at 1.6 m. Lines of best fit are $F_c = 2.57 + 0.410g_c - 0.0036g_c^2$, $n = 844$, $r^2 = 0.16$ for VPD < 1 kPa (+); $F_c = -7.17 + 2.520g_c - 0.0332g_c^2$, $n = 648$, $r^2 = 0.45$ for $1 \leq$ VPD < 2 kPa (×); and $F_c = -0.67 + 3.485g_c - 0.0713g_c^2$, $n = 84$, $r^2 = 0.12$ for VPD ≥ 2 kPa (●).

4.3.3 Responses of F_c to PPFD

Photosynthetic photon flux density (PPFD) was the most important determinant for daytime net canopy CO_2 flux density (Ruimy et al., 1995). Fig. 36 plots the hourly averaged net canopy CO_2 flux density against incident PPFD in daytime (PPFD > 0 μ mol m^{-2} s^{-1}) for the whole measurement period. Scatter in the F_c-light response curve for the entire growing period may be explained by in situ variations in the canopy structure (LAI and age) and microenvironmental variables (T_a and VPD) when the measurements were made (Figs. 37 to 39). The responses of F_c to incident PPFD were fitted with a rectangular hyperbolic model (Thornley, 1976; Pattey et al., 1991)

$$F_c\,(\mathrm{PPFD}) \;=\; \alpha\;\; \mathrm{PPFD} \,/\, (1 + \mathrm{PPFD}[\,\alpha\,/(F_{c2000} + R_d) - 1/2000]) - R_d \qquad (23)$$

where is α the initial slope of the fitted F_c-PPFD curve, usually referred to as the apparent light-use efficiency (Jones, 1992); F_{c2000} is the CO_2 flux density at PPFD = 2000 μ mol m^{-2} s^{-1}, a surrogate for the maximal net canopy CO_2 flux density; and R_d is the hypothetical mean dark respiration at PPFD = 0. F_c increased hyperbolically with PPFD. The coefficients of determination for this rectangular hyperbolic relationship are large implying that F_c over the ERC grassland is driven principally by PPFD (Table 4). The hyperbolic relationship between F_c and PPFD maintained throughout the growing season.

Because no water stress occurred at the ERC grassland, F_c did not display a tendency to saturate up to PPFD levels of 2000 μ mol m^{-2} s^{-1}, indicating that relatively higher levels of PPFD were required for light saturation in this well-watered grassland. In addition, with increasing solar radiation and wind speed, more PPFD will go inside the closed canopy where leaves are generally not light-saturated. This may also contribute to light-unsaturation for the grassland. The peak values of daytime F_c at

PPFD = 2000 μ mol m^{-2} s^{-1} appeared at the early closed canopy stage; thereafter F_c decreased as the grasses aged. The hypothetical mean dark respiration at PPFD = 0 (R_d) at the different growth stages was similar in magnitude to the median F_c values obtained at night with the EC technique (Table 4).

The initial slope was relatively constant (more than 0.05 μ mol CO_2 μ mol^{-1} PPFD) prior to the senescent period and dropped to less than 0.02 μ mol CO_2 μ mol^{-1} PPFD in the senescent period. The initial slope, the ratio of estimated mean dark respiration to daytime F_c at PPFD = 2000 μ mol m^{-2} s^{-1}, and the canopy light compensation point varied depending on the growth stages and generally increased with increasing air temperature and VPD (Table 6). This point confirms that the canopy gains carbon from the atmosphere under higher T_a and VPD regime at the expense of a relatively large respiratory loss. This is because higher VPD values generally render partial or complete closure of stomata leading to a decrease of CO_2 assimilation whereas higher temperatures may be more favorable to respiration (Kim and Verma, 1990b). Actually, effects from both VPD and temperature could not be readily separated owing to their close coupling. Note that the initial slope (α) values estimated from the hyperbolic model were larger than observed for other types of canopy (e.g. Baldocchi, 1994b; Friborg et al., 1997; Hollinger et al., 1994, 1998; Ruimy et al., 1995). This difference may be caused by the curvilinear nature of the F_c-PPFD response curve (Baldocchi et al., 1987) because linear regression analysis of the F_c-PPFD curves under lower PPFD regime gives very different results for α than did the rectangular hyperbolic model (Table 8); the linear fits were similar to reported values in the literature.

Estimated mean respiration rate (R_d = –6.78 μ mol m^{-2} s^{-1}, Table 6) from the F_c–PPFD curve when PPFD = 0 for the entire measurement period is compatible to those measured during the nighttime suggesting (R_N = –5.90 μ mol m^{-2} s^{-1} when T_a = 20 °C, Table 7) that we can use daytime F_c to get a reasonable estimates of the nighttime F_c (Ruimy et al., 1995).

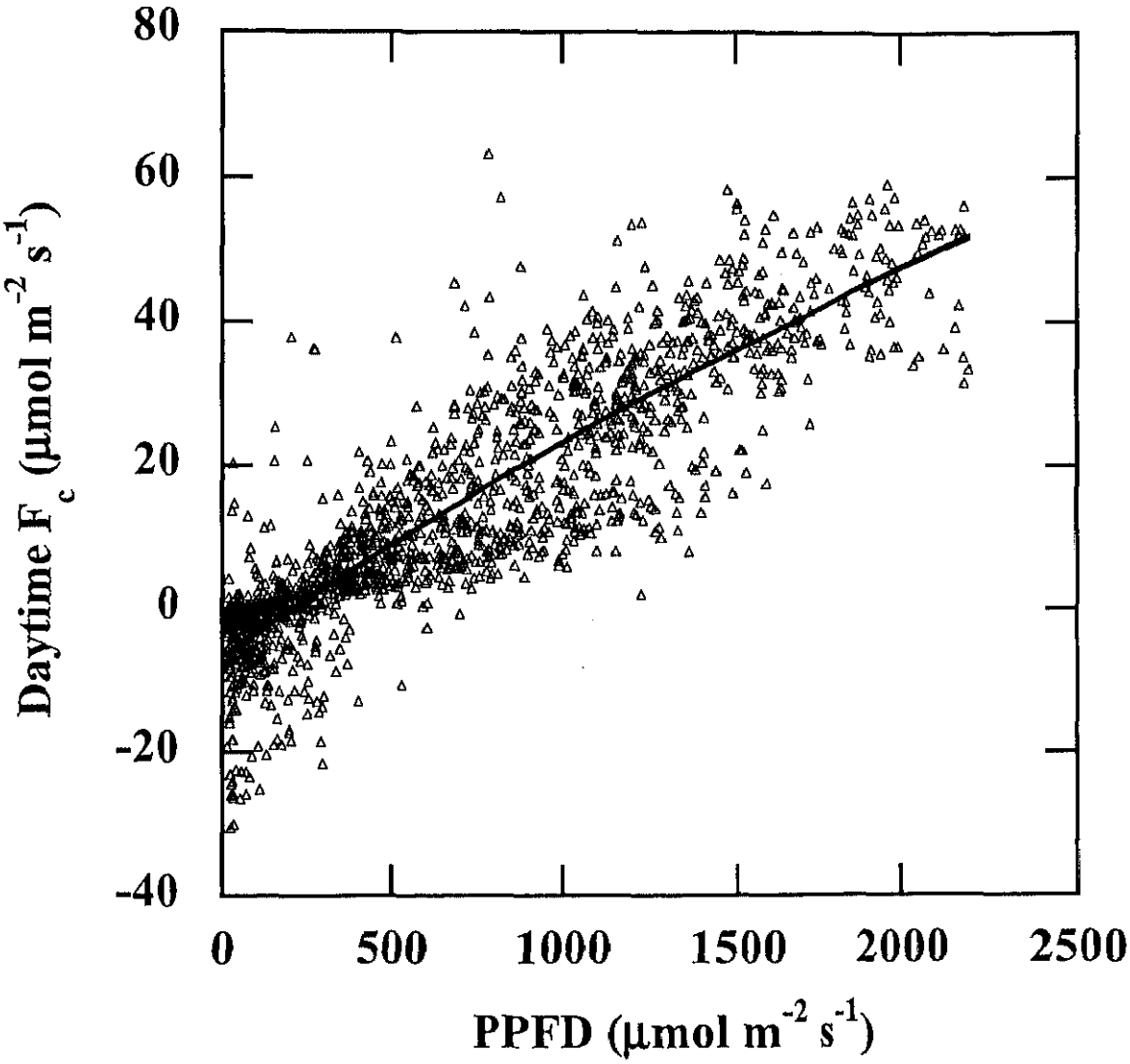

Figure 36. Relationships between net canopy CO_2 flux (F_c) and photosynthetic photon flux density (PPFD) for the entire measurement period. The data were fitted to a hyperbolic model and the best-fit model parameters are given in Table 6.

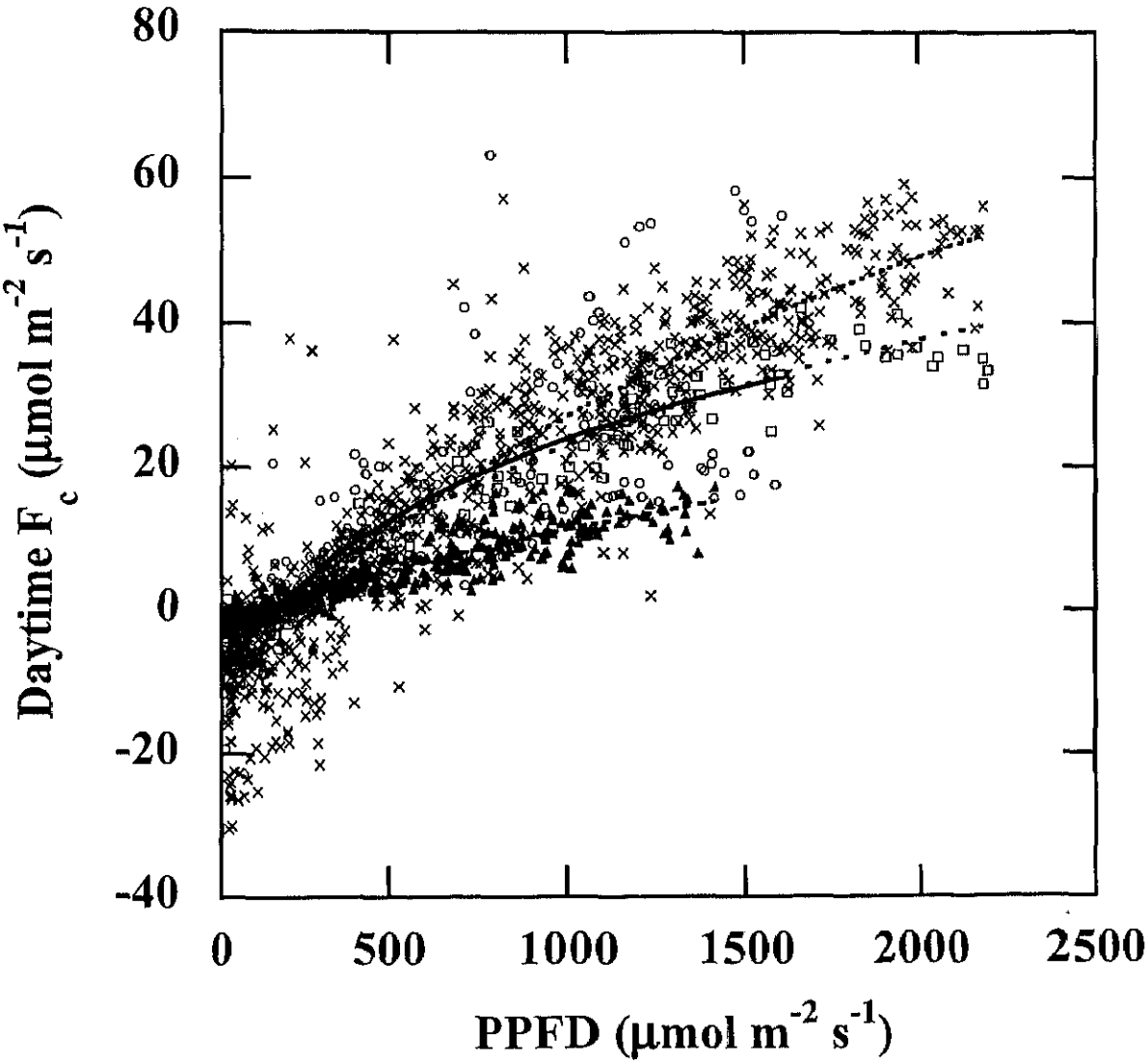

Figure 37. Relationships between net canopy CO_2 flux (F_c) and photosynthetic photon flux density (PPFD) for various growth stages of the ERC grassland: The rapid growth period (□), the closed canopy period (×), the flowering period (○), and the senescent period (▲). The data were fitted to a hyperbolic model and the best-fit model parameters are given in Table 6.

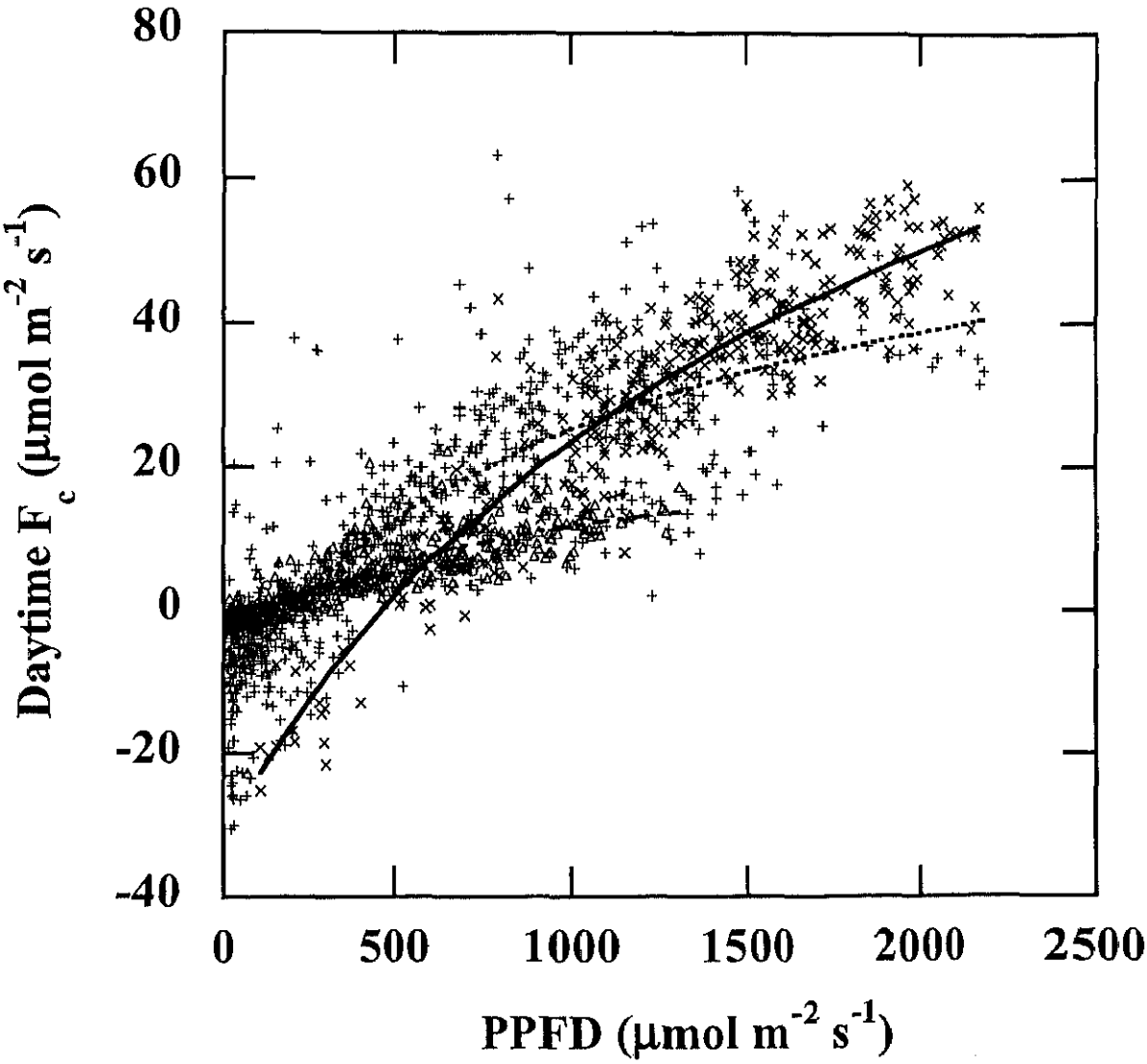

Figure 38. Relationships between net canopy CO_2 flux (F_c) and photosynthetic photon flux density (PPFD) under different air temperatures (T_a), $T_a < 10$ °C (○), $10 \leq T_a < 20$ °C (△), $20 \leq T_a < 30$ °C (+), and $T_a \geq 30$ °C (×). The data were fitted to a hyperbolic model and the best-fit model parameters are given in Table 6.

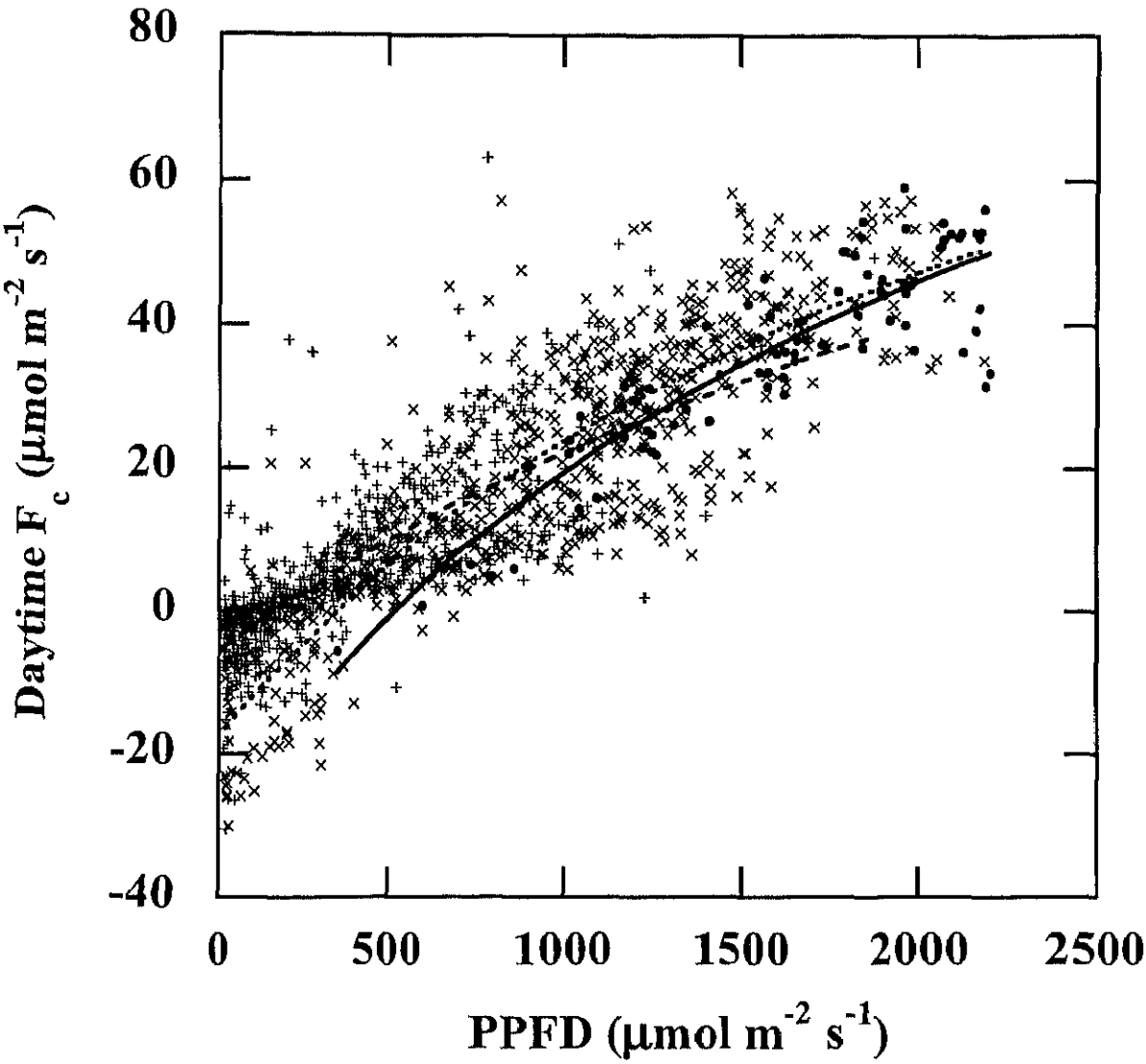

Figure 39. Relationships between net canopy CO_2 flux (F_c) and photosynthetic photon flux density (PPFD) under different vapor pressure deficits (VPD), VPD < 1 kPa (+), 1 ≤ VPD < 2 kPa (×), and VPD ≥ 2 kPa (●). The data were fitted to a hyperbolic model and the best-fit model parameters are given in Table 6.

Table 6 Characteristics of the rectangular hyperbolic responses of hourly net canopy CO_2 flux (F_c) to incident hourly photosynthetic photon flux density (PPFD) in the daytime. α, the initial slope in mol CO_2 mol^{-1} photon; F_{c2000}, F_c at PPFD = 2000 μ mol m^{-2} s^{-1}; R_d, the mean dark respiration estimated from the F_c-PPFD curve; η, the R_d-to-F_{c2000} ratio; n, numbers of observations; r^2, the coefficient of determination; and LCP, the estimated canopy light compensation point. The same data were separately grouped according to the growth stages, air temperature regime (T_a) and vapor pressure deficit (VPD).

Treatment	LAI	α	F_{c2000}	R_d	η	n	r^2	LCP
		mol mol^{-1}	μ mol m^{-2} s^{-1}					μ mol m^{-2} s^{-1}
Rapid growth period	2.13	0.047±0.004	37.72±0.79	−7.48±0.80	0.20	133	0.94	174.1
Closure period	5.50	0.052±0.003	49.13±0.83	−11.15±0.76	0.23	846	0.83	232.5
Flowering period	5.37	0.058±0.013	36.21±2.84	−8.25±1.83	0.23	220	0.62	160.6
Senescence period		0.018±0.002	19.58±1.06	−2.45±0.29	0.13	377	0.83	142.3
Entire growth period	2.1–5.5	0.033±0.002	47.69±0.80	−6.78±0.47	0.14	1576	0.78	210.0
T_a <10 °C	2.1–5.5	0.036±0.022	10.16±4.55	−3.70±1.20	0.36	44	0.54	131.0
10 ≤ T_a < 20 °C	2.1–5.5	0.033±0.005	16.73±1.35	−4.10±0.57	0.25	391	0.62	143.6
20 ≤ T_a < 30 °C	2.1–5.5	0.067±0.006	38.83±1.17	−11.13±0.90	0.29	819	0.71	193.1
T_a ≥30 °C	2.1–5.5	0.083±0.009	50.07±0.74	−30.95±2.73	0.62	322	0.87	463.5
VPD <1 kPa	2.1–5.5	0.035±0.003	40.36±3.10	−5.51±0.54	0.14	844	0.59	164.2
1 ≤ VPD < 2 kPa	2.1–5.5	0.057±0.005	47.38±1.12	−17.53±1.49	0.37	648	0.75	348.0
VPD ≥ 2 kPa	2.1–5.5	0.070±0.027	46.21±0.97	−29.93±11.07	0.65	84	0.81	521.0

4.3.4 Nighttime F_c

The canopy emits CO_2 to the atmosphere due to respiration from plants and soil throughout the day. On a daily basis, net carbon losses from the canopy accounted for about 20 to 65 % of net carbon gains from the air during the growing season (Table 4). Therefore, a better understanding of the nighttime F_c is essential for understanding the canopy-atmosphere carbon exchange (Baldocchi et al., 1997b; Ryan et al., 1997).

Generally, dark respiration of the canopy is dependent on temperatures (Fig. 40) and can be evaluated with the observed nighttime F_c (Ruimy et al., 1995). We employed an exponential function (Hollinger et al., 1994) to describe the responses of nighttime F_c to temperatures when wind speed was higher than 0.5 m s^{-1}

$$R_N = R_{N0}\, Q_{10}^{(T - To)/10} \qquad (24)$$

where R_N is canopy nighttime respiration (net canopy CO_2 flux density at night); R_{N0} is the respiration at a reference temperature T_0; Q_{10} is the temperature coefficient, the respiration rate change with a 10 °C increase in temperature. Because of shading by the plants and mulching by the litter, variations in soil temperature (T_s) were usually lower than those in air temperature (T_a). In this case, dark respiration may be more affected by T_a than T_s, at least for plant respiration (Table 7). The Q_{10} was 4.9 when calculated with T_a, and 3.9 when calculated using soil temperature (Table 7). The values of Q_{10} varied depending on the growth stage of the canopy. Under higher VPD and T_a, generally during the closed canopy period, the canopy dark respiration increased substantially with air temperature with a Q_{10} value of 7.7. Nighttime F_c was poorly related to T_a ($r^2 = 0.01$) during the senescent period presumably because of poor fetch. Q_{10} for T_a for the whole measurement period, 4.9, was similar to the Q_{10} value of 4.6 reported by Valentini et al. (1995) for a serpentine grassland.

A positive linear relationship existed between nighttime net CO_2 flux density and sensible heat flux density (Fig. 41), indicating that atmospheric turbulent events at night may affect nighttime F_c measurements over the canopy by EC technique (Hollinger et al., 1994; Kelliher et al., 1999; Lee et al., 1997, 1999).

Estimated values of the canopy respiration (R_d) from the daytime F_c-PPFD curves when PPFD = 0 were slightly larger than those (R_N) from the nighttime F_c-T curves when wind speed was higher than 0.5 m s^{-1} (Tables 6 and 7). This is due to the fact that the EC technique usually underestimates fluxes in stable conditions (Baldocchi et al., 1997b; Goulden et al., 1996b; Hollinger et al., 1994; Jarvis et al., 1997). Nevertheless, we may use either R_d or R_N to estimate soil and plant respiration.

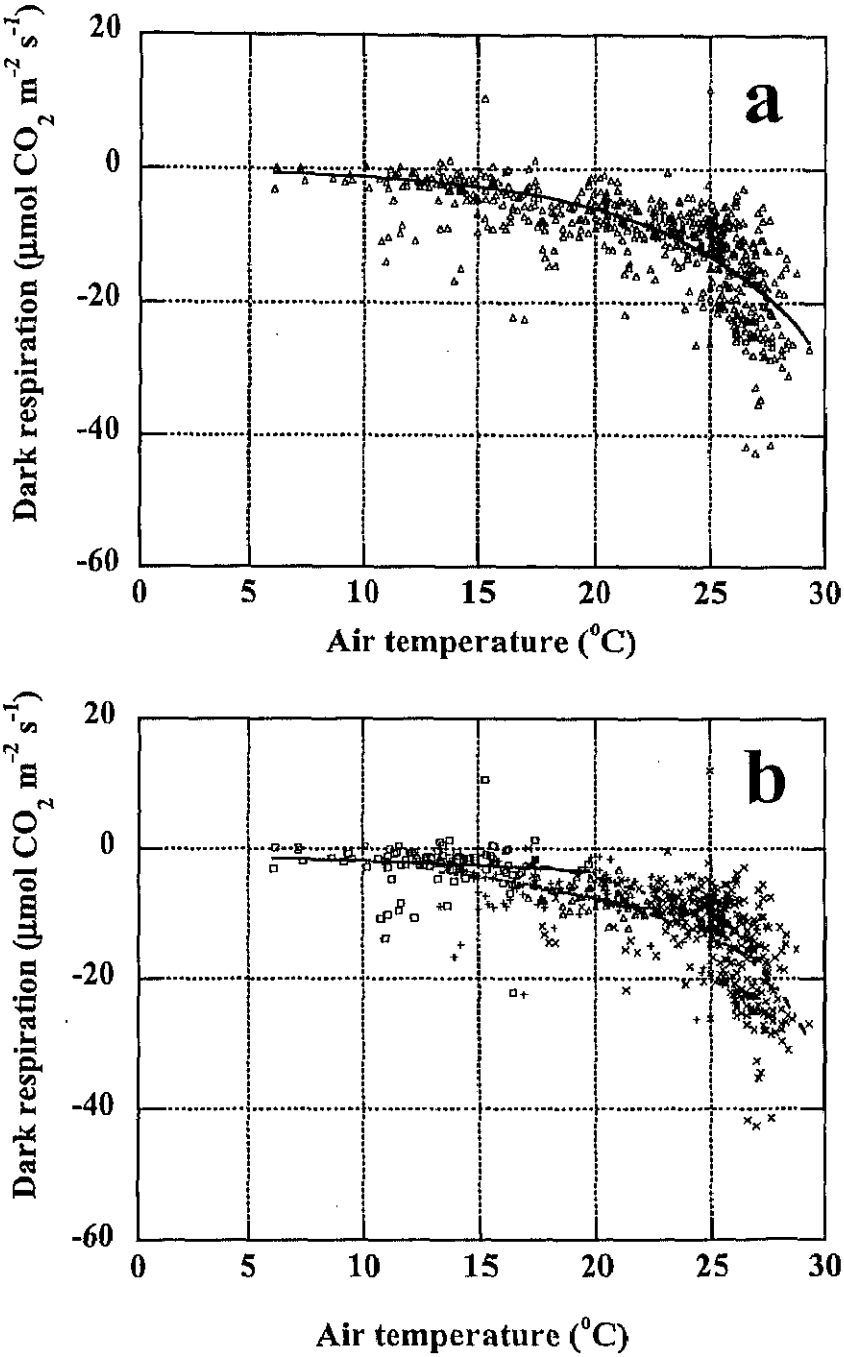

Figure 40. Relationships between nighttime net canopy CO_2 flux (F_c) and air temperature (T_a). a: For the entire measurement period. b: For the rapid growth period (△), the closed canopy period (×), the flowering period (+), and the senescent period (□). The data were fitted to an exponential model and the best-fit model parameters are given in Table 7.

Table 7 Summary of nighttime net canopy CO_2 flux (F_c) in response to temperature (T in °C) in terms of an exponential function when wind speeds were greater than 0.5 m s^{-1}. Q_{10}, the temperature coefficient; R_N in μ mol m^{-2} s^{-1}, the mean dark respiration estimated from the nighttime F_c-T curve; n, numbers of observations; r^2, the coefficient of determination; T_a, 1.6-m air temperature; and T_s, 2-cm soil temperature.

Growth stage	LAI	Q_{10}	R_N (T = 10)	R_N (T = 20)	R_N (T = 30)	n	r^2
Rapid growth period (T_a)	2.13	2.4±0.5	−3.21±0.71	−7.63±0.26	−18.14±3.56	50	0.27
Closure period (T_a)	5.50	7.7±1.2	−0.57±0.14	−4.40±0.42	−33.99±2.02	400	0.37
Flowering period (T_a)	5.37	3.2±0.6	−2.43±0.56	−7.71±0.53	−24.45±4.74	94	0.24
Senescence period (T_a)		1.9±1.4	−1.89±0.66	−3.52±1.70	−6.56±7.86	99	0.01
Entire growth period (T_a)	2.1–5.5	4.9±0.4	−1.20±0.16	−5.90±0.31	−28.95±1.18	643	0.52
Entire growth period (T_s)	2.1–5.5	3.9±0.5	−1.26±0.24	−4.97±0.41	−19.64±0.84	643	0.33

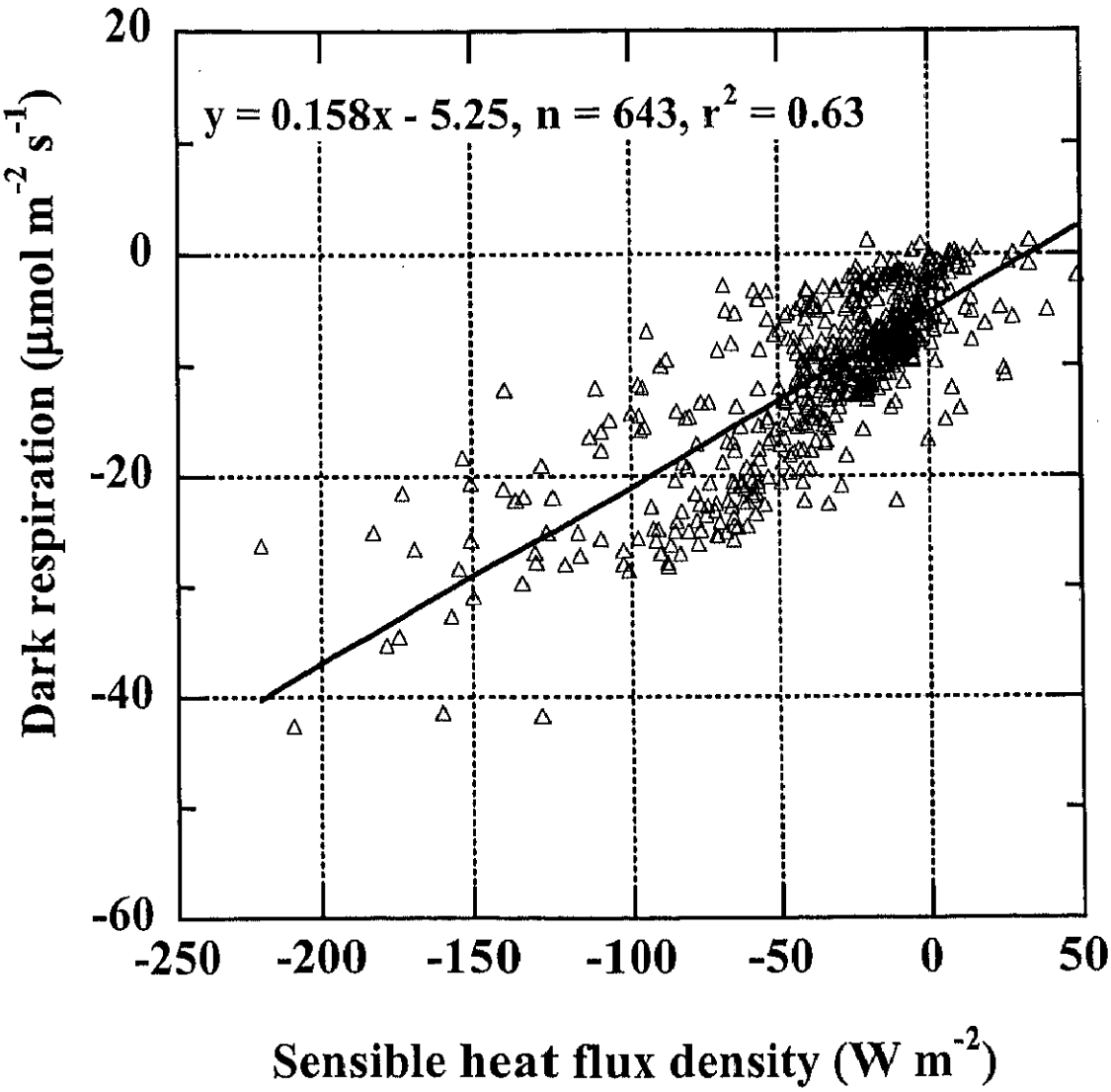

Figure 41. The relationship between nighttime net canopy CO_2 flux (F_c) and the sensible heat flux density (H). The best-fit line is F_c (μ mol m^{-2} s^{-1}) = 0.158H (W m^{-2}) – 5.25, n = 643, r^2 = 0.63.

4.3.5 Water use efficiency and its affecting factors

Generally, WUE of the canopy is associated with PPFD and VPD under well-watered conditions (Baldocchi et al., 1985; Zur and Jones, 1984). Under lower PPFD regime (PPFD < 800 μ mol m^{-2} s^{-1}), WUE was relatively independent of PPFD (Fig. 42a). The canopy, however, used water more efficiently under lower PPFD and low VPD. When PPFD was larger than 1000 μ mol m^{-2} s^{-1}, WUE tended to decrease with increase of PPFD. This may be caused by higher water losses from the soil and plants due to higher VPD. WUE tended to decrease with increase in VPD. As VPD exceeded 2 kPa, WUE was markedly decreased (Fig. 42b). This may be due to VPD-induced partial stomatal closure, which may lead to a lower F_c while ET was still relatively high due to a strong dependence of ET on VPD (Jarvis and McNaughton, 1986). Baldocchi (1994b) reported similar linear responses of WUE to VPD for a wet wheat canopy.

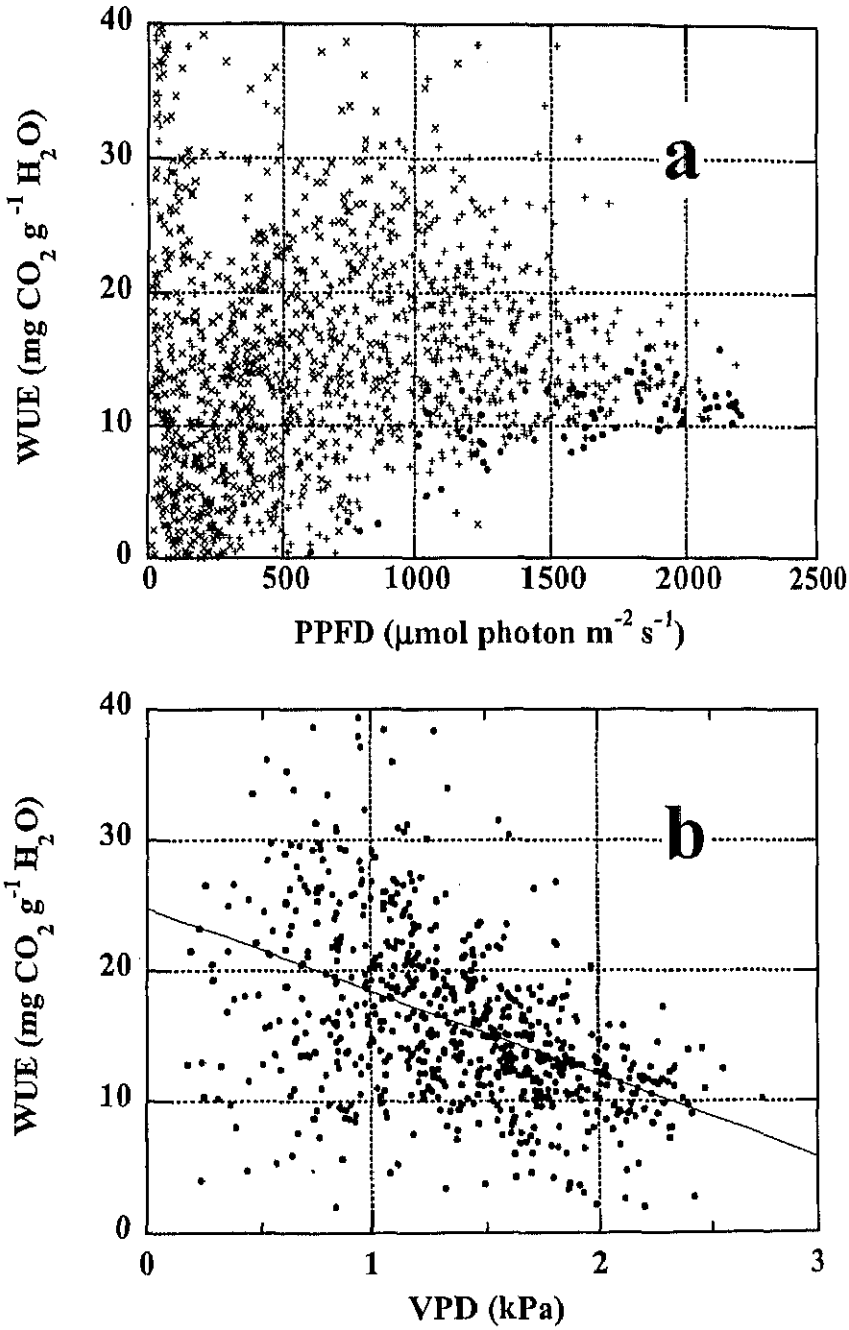

Figure 42. a: The relationship between water use efficiency (WUE) and photosynthetic photon flux density (PPFD). Data are grouped according to vapor pressure deficit (VPD): VPD < 1 kPa (○), 1 ≤ VPD < 2 kPa (+), and VPD ≥ 2 kPa (●). b: The relationship between WUE and VPD. Only data when solar radiation was larger than 300 W m^{-2} are included, and the regression line is WUE = 24.77 – 6.36VPD, n = 774, r^2 = 0.22.

4.4 Comparisons with leaf level fluxes

Physiological based models generally attempt to scale flux measurements up from individual leaves to canopies, then to regions, or even to the globe. Clearly, a better understanding of the basic features of leaf-scale fluxes is very important in this up-scaling process. Additionally, measurements of leaf-scale fluxes help reveal the features of canopy-scale flux.

Canopy-scale CO_2 flux is closely related with leaf-scale CO_2 flux (photosynthesis) in terms of leaf area index. Flux measurements over the canopy made by the EC technique are compared with those made with LI-6400 porometers on individual leaves of dominant species that composed the canopy (Figs. 43 to 48, Tables 8 and 9). LAI was about 5.54 and SWC was 0.40 when the measurements were made. SWC was about 45%. Net canopy scale CO_2 flux density (F_c) is expressed in unit of per ground area while net leaf-scale CO_2 flux density (P_n) is in unit of per leaf area.

P_n on individual leaves did not follow PPFD closely as that over the canopy. F_c was about two to three times P_n (Fig. 43). When normalized with LAI, however, F_c was lower in magnitude than that P_n of individual leaves. This is reasonable because the canopy was composed of leaves of C3 and C4 species with different photosynthetic capacities whereas the measured leaves were very healthy and vigorous in photosynthesis. P_n of *Solidago altissima* (C3) was about half of P_n of *Imperata cylindrica* (C4). ET (TR) and g_s paralleled in daytime trends (Fig. 44).

WUE (F_c/ET) of the canopy was more similar in daytime sequence and magnitude to WUE (P_n/TR) of *I. cylindrica* than to that of *S. altissima* because the canopy was dominated by C4 species during the measurements (Fig. 45). WUE of the canopy peaked in the mid-morning and diminished throughout the rest of the daytime (Fig. 35). It could not recover in the late afternoon as did on individual leaves presumably due to the occurrence of sensible heat advection that may substantially enhance ET. WUE (P_n/TR)

of *S. altissima* was significantly lower than that of *I. cylindrica*.

Leaf conductances observed for *S. altissima* were approximately twice as high as those for *I. cylindrica*. Furthermore, the estimated stomatal conductance from the Penman-Monteith model (Table 5) was very similar to that observed on individual leaves of C4 species (Fig. 44) during the C4-dominated canopy closure period (DOY 204 to 255).

Leaf temperatures (T_l) were slightly higher than air temperature (T_a), and leaf surface vapor pressure deficit (VPD_l) were higher than atmospheric VPD (Fig. 46). In comparison with ambient CO_2 concentration at 2 m (Ca_{hi}), the CO_2 concentration at 0.25 m (Ca_{lo}) was higher throughout nighttime, lower after sunrise because of photosynthesis, and nearly identical in the afternoon due to strong turbulent mixing (Fig. 47). Variations in CO_2 profile were tightly coupled with F_c. Intercellular CO_2 concentrations (Ci) were higher for *S. altissima* than for *I. cylindrica*.

Measurements on individual leaves of dominant species at the study site indicated that *S. altissima* (C3) and *Festuca arundinacea* (C3) light-saturated at up to 1000 μ mol m^{-2} s^{-1} levels of PPFD while *I. cylindrical* (C4) and *Miscanthus sinensis* (C4) did not exhibit light saturation even at 1800 μ mol m^{-2} s^{-1} of PPFD (Fig. 48). For the canopy, no light-saturation were clearly demonstrated, during the canopy closure period and the flowering period (Fig. 37). This may be because C4 species dominated the canopy when the measurements were performed.

Generally, the initial slope for individual leaves is higher than for the canopy (Baldocchi, 1994b). The hyperbolic modeling results in the present study indicate that the initial slope for the canopy was on the same order of magnitude as those for the individual leaves (Tables 6 and 8). Therefore, the canopy was very efficient in light-use. This point can be also mirrored by relatively higher water use efficiency of the canopy (Table 4). The canopy light compensation point was 4 to 6 times the leaf light compensation point (Tables 6 and 8).

The initial slopes and the hypothetical mean dark respiration estimated from the

linear modeling of the F_c/P_n-PPFD response relationship under weak PPFD regime was generally smaller than those obtained from the hyperbolic model (Tables 6, 8 and 9). However, the linear modeling results might be more reasonable because they excluded the effect of curvilinear nature of the hyperbola (Baldocchi et al., 1987). Additionally, the initial slope for the canopy was very similar to those for the individual leaves of C4 under weak PPFD regime during the canopy closure period when C4 species dominated (Table 9).

If we assume that a typical value of leaf respiration is $-1.26\ \mu$ mol m^{-2} s^{-1} (on leaf area) during the canopy closure period (Table 9), and then extend this value to the canopy scale by multiplying LAI of 5.34, we get a value of *ca.* $6.73\ \mu$ mol m^{-2} s^{-1} (on ground area), which is about 65% of the hypothetical mean dark respiration ($10.39\ \mu$ mol m^{-2} s^{-1}) of the canopy. Although this percentage may be overestimated, otherwise, it indicates that the fraction of plant respiration at the ERC grassland is substantial.

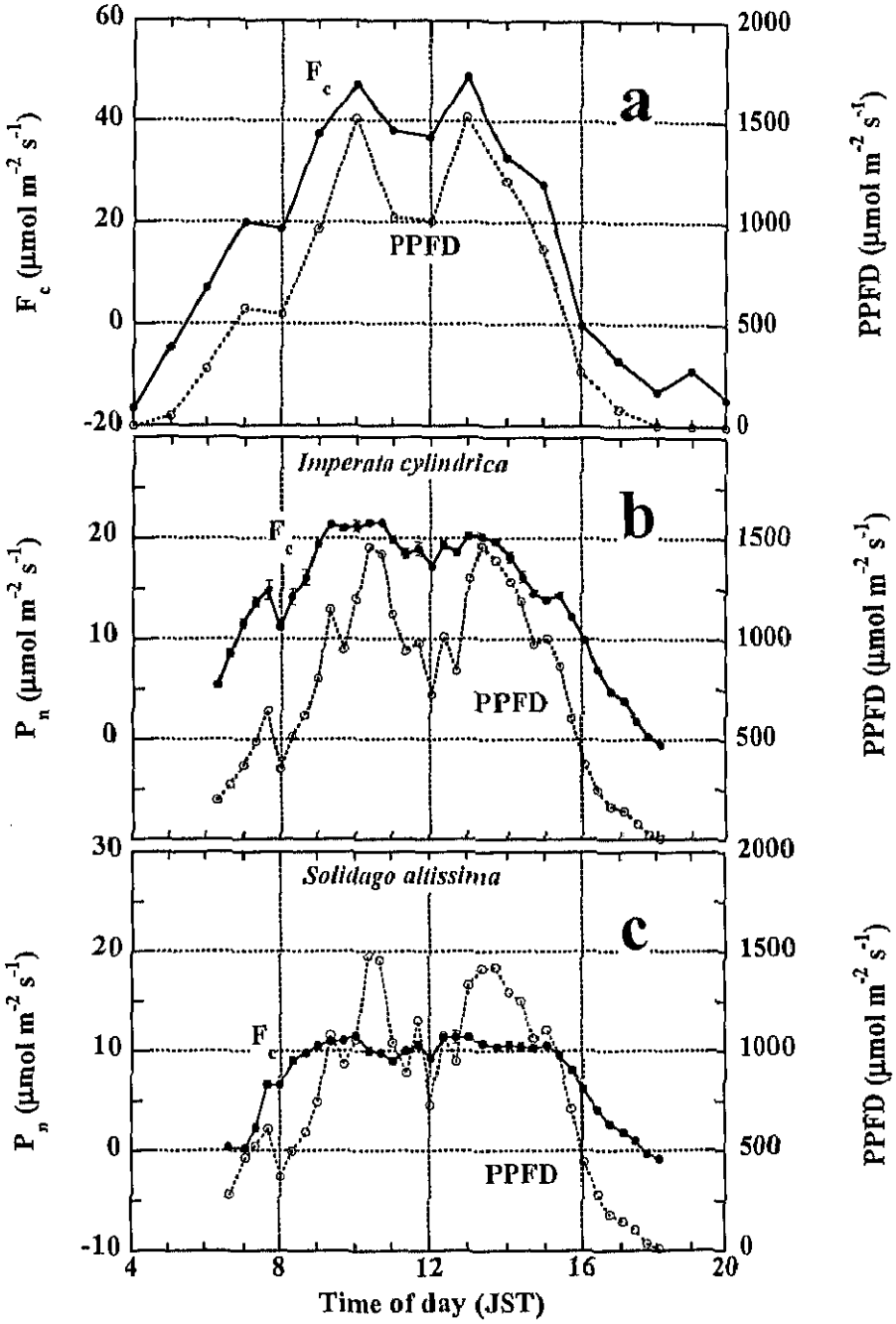

Figure 43. Comparisons of the daytime sequence between the canopy-scale and leaf-level flux measurements on 30 August 1999. a: the canopy; b: *Solidago altissima* (C3); c: *Imperata cylindrical*. The canopy-level CO_2 flux (F_c) was measured by the EC techniques and the data was hourly averaged. The leaf-level CO_2 fluxes (P_n) were measured with LI-6400 porometers, and the data were sampled at 2 min interval and averaged over 20 min. Vertical bars indicate standard errors.

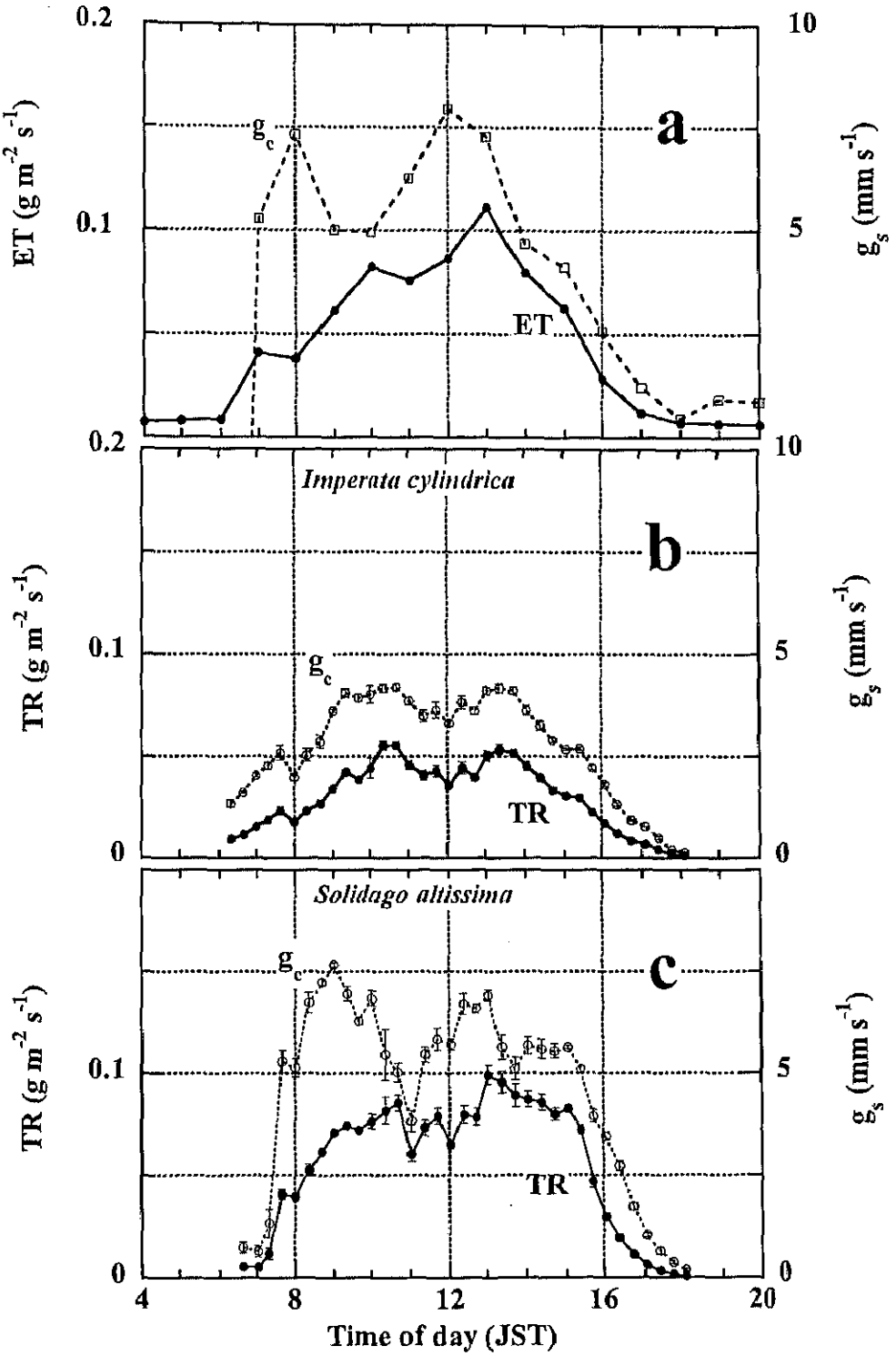

Figure 44. Same as Fig. 43 but for stomatal conductance (g_s), evapotranspiration (ET) and transpiration (TR). The stomatal conductance for the canopy was estimated from the Penman-Monteith combination equation.

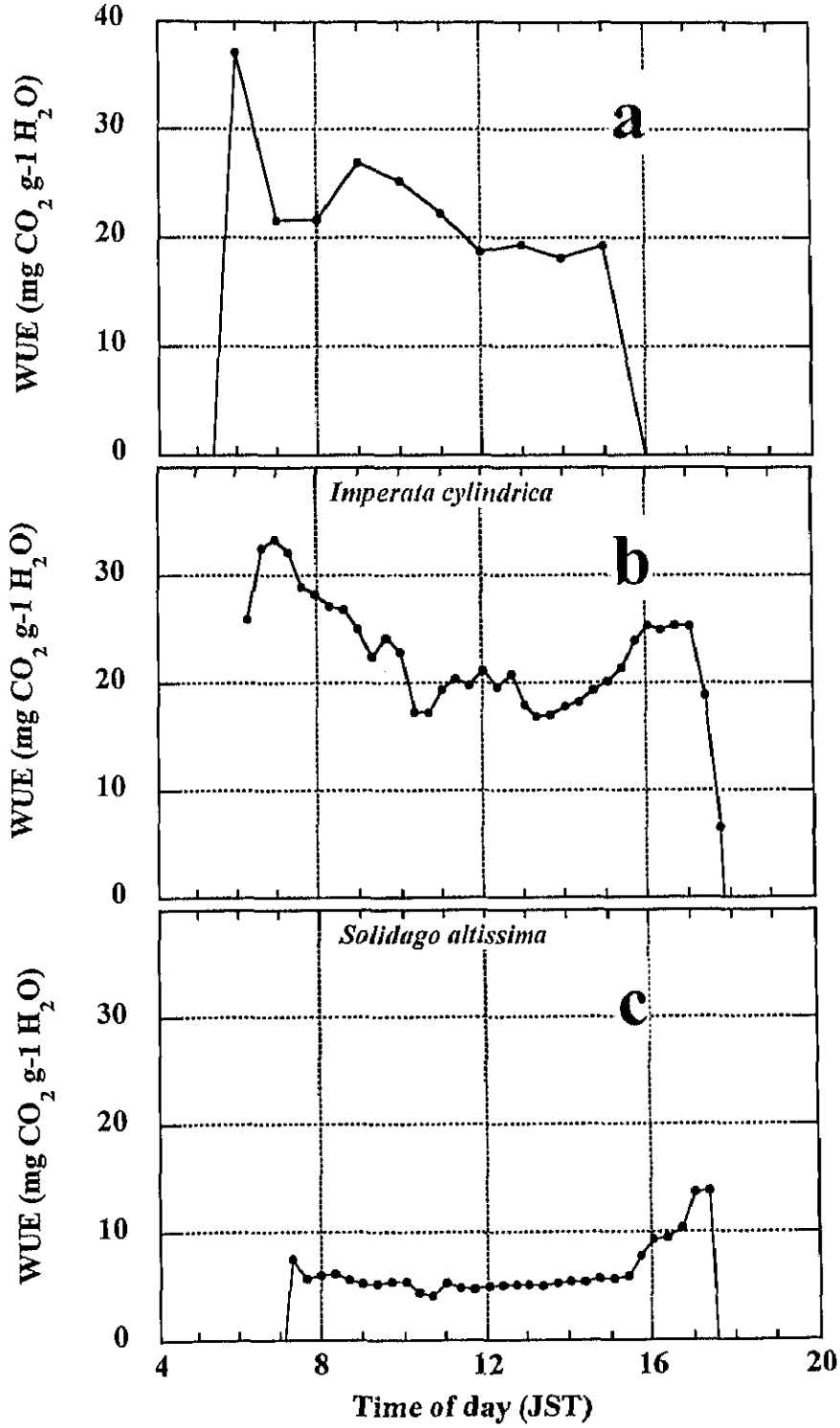

Figure 45. Same as Fig. 43 but for water use efficiency (WUE).

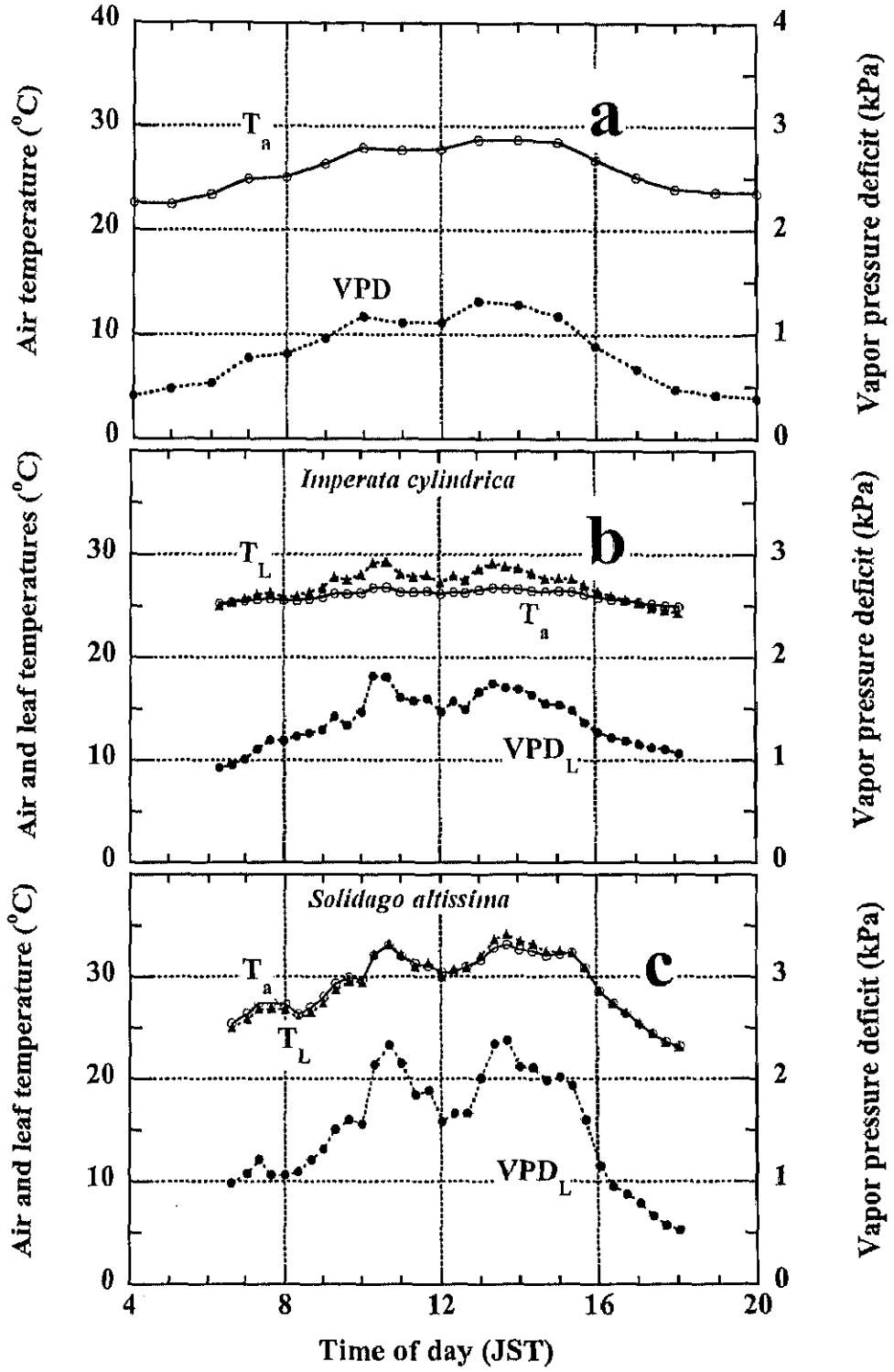

Figure 46. Same as Fig. 43 but for air temperature (T_a), leaf temperature (T_l), atmospheric vapor pressure deficit (VPD) and leaf-surface vapor pressure deficit (VPD_l).

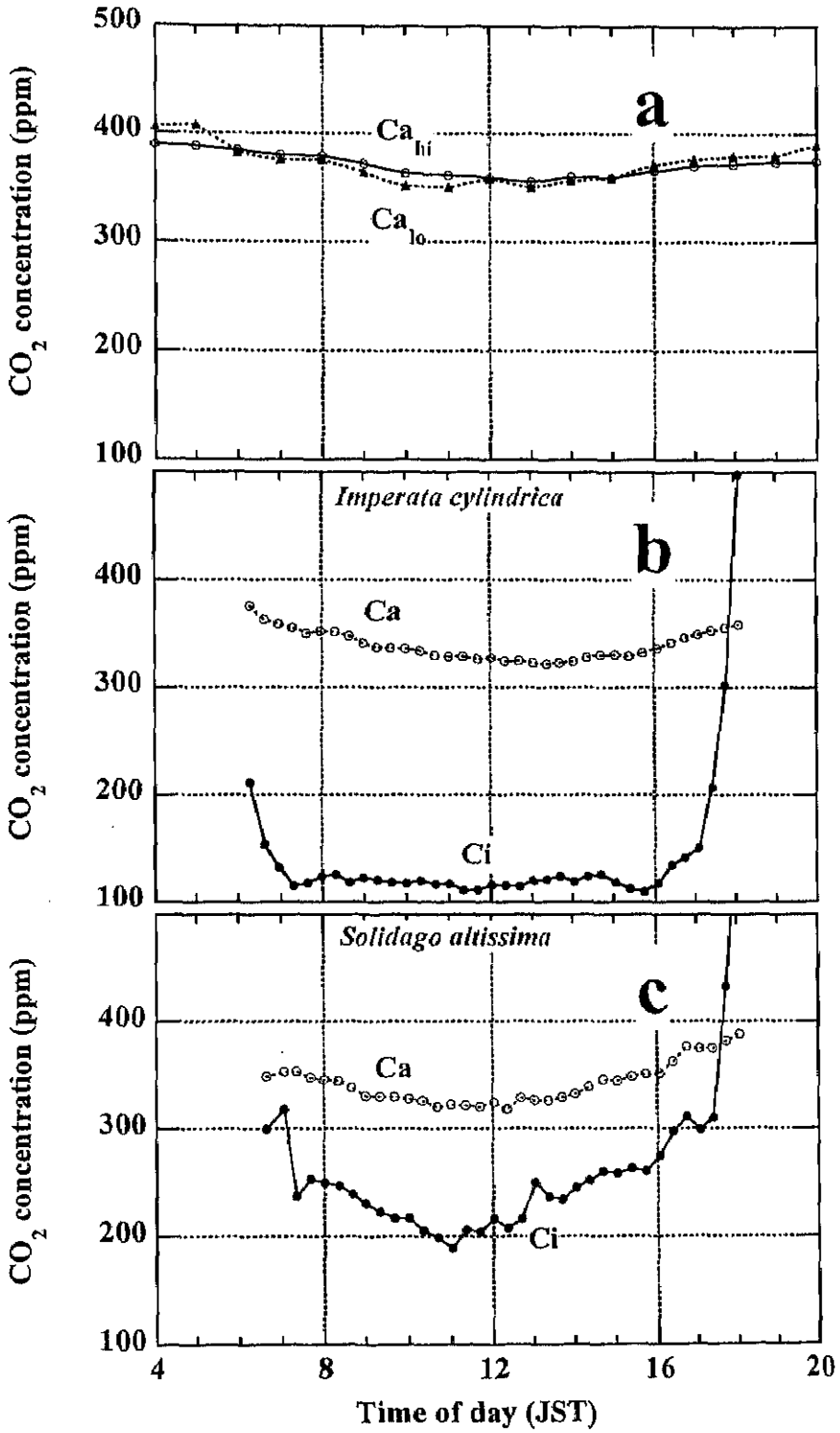

Figure 47. Same as Fig. 43 but for atmospheric CO_2 concentration (Ca_{hi} at 2 m, Ca_{lo} at 0.25 m) and intercellular CO_2 concentration (Ci).

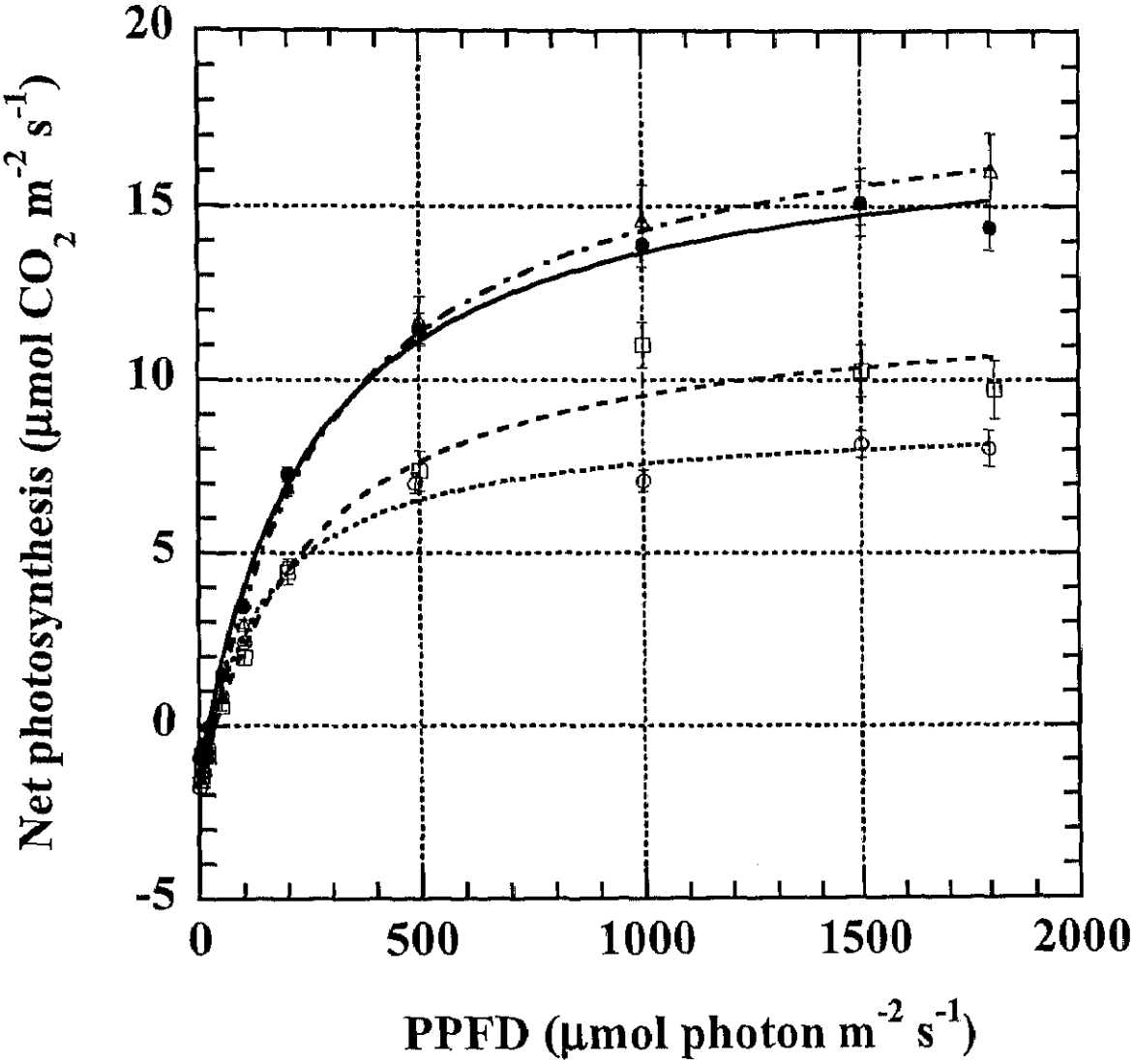

Figure 48. Relationships between net leaf CO_2 flux density (P_n) and incident photosynthetical photon flux density (PPFD). *Solidago altissima* (○), *Festuca arundinacea* (□), *Imperata cylindrical* (△), and *Miscanthus sinensis* (●). The data were fitted to a hyperbolic model identical to with that for the canopy and the best-fit model parameters are given in Table 8.

Table 8 Relationship between net leaf CO_2 flux (P_n) and incident photosynthetic photon flux density (PPFD) modeled with a rectangular hyperbolic function (as was done for the canopy) for 4 dominant species (*Solidago altissima, Festuca arundinacea, Imperata cylindrical* and *Miscanthus sinensis*). The model coefficients were α_l, the initial slope; P_{n2000}, P_n at PPFD = 2000 μ mol m^{-2} s^{-1}; R_l, the mean dark respiration of leaves estimated from the P_n-PPFD curve; η, R_l-to-P_{n2000} ratio; n, number of replicate measurements; r^2, the coefficient of determination; LCP, the estimated leaf light compensation point. The ambient CO_2 concentration (C_a), cuvette leaf temperature (T_l) and leaf-air vapor pressure deficit (VPD_l) are also presented. Subscript *l* is for leaf.

Species	α_l	P_{n2000}	R_l	η	n	r^2	LCP_l	C_a	T_l	VPD_l
	mol mol^{-1}	μ mol m^{-2} s^{-1}					μ mol m^{-2} s^{-1}	ppm	°C	kPa
S. altissima	0.074±0.008	8.21±0.18	−1.77±0.18	0.22	8	1.00	28.7	369	31.8	1.9
F. arundinacea	0.056±0.011	10.82±0.43	−1.76±0.37	0.16	7	0.99	35.9	355	31.8	3.4
I. cylindrica	0.074±0.006	16.31±0.25	−1.99±0.21	0.12	9	1.00	29.7	357	31.0	2.7
M. sinensis	0.073±0.007	15.36±0.29	−1.26±0.24	0.08	9	1.00	18.5	369	31.1	2.1
Average	0.069±0.008	12.68±0.29	−1.70±0.25	0.16	33	1.00	28.2	363	31.4	2.5

Table 9 The linear model coefficients under low PPFD (200 μ mol m^{-2} s^{-1} for leaves and 500 μ mol m^{-2} s^{-1} for the canopy). Meanings of symbols are the same as those in Tables 6 and 8.

Treatment	α	R_d	r^2	LCP
	mol mol^{-1}	μ mol m^{-2} s^{-1}		μ mol m^{-2} s^{-1}
Rapid growth period	0.036	−6.54	0.77	182.9
Closure period	0.042	−10.39	0.33	244.6
Flowering period	0.037	−5.59	0.54	150.3
Senescence period	0.015	−2.21	0.56	144.6
Entire growth period	0.033	−6.82	0.35	209.6
T_a <10 °C	0.018	−2.86	0.43	155.2
10 ≤ T_a < 20 °C	0.021	−2.93	0.51	141.9
20 ≤ T_a < 30 °C	0.044	−9.67	0.48	222.2
T_a ≥30 °C	0.054	−26.13	0.50	484.2
VPD <1 kPa	0.032	−5.26	0.41	164.6
1 ≤ VPD < 2 kPa	0.053	−18.24	0.48	342.4
VPD ≥ 2 kPa	0.028	−8.88	0.79	318.8

Species	α_l	R_l	r^2	LCP_l
	mol mol^{-1}	μ mol m^{-2} s^{-1}		μ mol m^{-2} s^{-1}
S. altissima	0.031	−1.25	0.97	40.3
F. arundinacea	0.030	−1.38	0.98	46.0
I. cylindrica	0.043	−1.56	1.00	36.3
M. sinensis	0.041	−0.86	1.00	21.0
Average	0.036	−1.26		35.9